Electronic Supplementary Material (ESI) for Inorganic Chemistry Frontiers.

Supporting Information

Precisely tuning resorcin[4]arene-based metal-organic dimers with highly dispersed palladium nanoparticles for nitroaromatic hydrogenation in water

Fei-Fei Wang, [a,b] Wei Jiang ,[c] Wen-Yuan Pei [a]* and Jian-Fang Ma [a]*

[a] *Key Laboratory of Polyoxometalate and Reticular Material Chemistry of Ministry of Education, Department of Chemistry, Northeast Normal University, Changchun 130024, China*

[b] *Department of Chemistry, Xinzhou Normal University, Xinzhou 034000, China*

[c] *Key Laboratory of Preparation and Application of Environmental Friendly Materials, Ministry of Education, Jilin Normal University, Changchun 130103, China*

* Correspondence authors

E-mail: peiwy527@nenu.edu.cn (W.-Y. Pei)

E-mail: majf247@nenu.edu.cn (J.-F. Ma)

Experimental section

Material and methods. Zinc nitrate hexahydrate ($Zn(NO_3)_2 \cdot 6H_2O$), 1,4-benzenedicarboxylic acid, 2-aminoterephthalic acid, 2-nitroterephthalic acid, 2,6-naphthalenedicarboxylic acid, 4,4'-biphenyldicarboxylic acid, 4,4'-stilbenedicarboxylic acid, azobenzene-4,4'-dicarboxylic acid, Palladium chloride ($PdCl_2$), 50% Hydrazine hydrate, Ammonia borane (NH_3BH_3), Chlorobenzene and a series of nitroaromatic compounds were purchased from Aladdin Industrial Co., Ltd. 2,2'-bipyridine-5,5'-dicarboxylic acid and *p*-terphenyl-4,4"-dicarboxylic acid were offered by Jinan Henghua Sci. & Tec. Co. Ltd. , Ltd. *N*,*N*'-dimethylformamide (DMF) was obtained from Tianjin Fuyu Chemical Reagents Company. Methanol was HPLC grade. Tetra(imidazole)resorcin[4]arene (TIC4R) was prepared according to the literature method.[1] PXRD patterns were performed on a Rigaku Dmax 2000 X-ray diffractometer and Rigaku SmartLab X-ray diffractometer with graphite monochromatized CuKα radiation (λ = 0.154 nm). Perkin-Elmer Model TG-7 analyzer was used to measure thermogravimetric curves. FT-IR spectrum was determined on a Nicolet 6700 FT-IR spectrometer with a KBr plate. Field emission scanning electron microscope (FESEM, Philips XL-30) was employed to record the morphologies of the materials. Elemental analytical data of C, H and N were recorded on a PerkinElmer 2400 CHN elemental analyzer. Leeman Laboratories Prodigy inductively coupled plasma−optical atomic emission spectrometer (ICP−AES) was used to record the content of Pd. Conversion and selectivity were determined with high performance liquid chromatography (HPLC) with an Inertsil (5 μm, 4.6×150 mm) ODS C18 column using a UV−vis detector at λ = 254 nm (Agilent-1220). ^{1}H NMR spectrum was recorded on a Varian 500 MHz. ESCA LAB spectrometer (USA) with a monochromatic Al Kα source (hν 1486.6eV) was applied to determine X-ray photoelectron spectroscopy (XPS). High-resolution transmission electron microscopy (HRTEM) image was achieved on a JEOL 2100F with an accelerating voltage of 200 kV.

X-ray crystallography. Crystallographic data of **1-9** were collected on an Oxford Diffraction Gemini R Ultra diffractometer with graphite-monochromated MoKα radiation (λ = 0.71073 Å). Structures of **1-9** were solved by direct methods with SHELXS-2018/3 and refined on F^2 by full-matrix least-squares with SHELXTL-2018/3 within WINGX.[2-4] Multi-scan method was applied for absorption corrections. Non-hydrogen atoms were refined anisotropically. SQUEEZE function in PLATON was employed to refine the structures of **4**, **5** and **9**, and their formulas were obtained on the basis of the diffused electron

density, thermogravimetric analysis and elemental analysis.[5] Crystallographic data were listed in Table S2. Selected bond lengths and angles were given in Tables S3-S11.

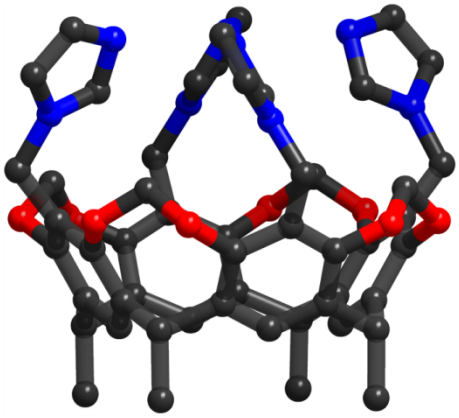

Scheme S1. Structure of ligand TIC4R.

Synthesis of $[Zn_4(TIC4R)_2\cdot(L^1)_2\cdot(OH)_2]\cdot 2HCOO\cdot 4DMF$ (1). A mixture of TIC4R (9 mg, 0.010 mmol), $Zn(NO_3)_2\cdot 6H_2O$ (14 mg, 0.047 mmol) and H_2L^1 (7 mg, 0.042 mmol) was added to a solution of DMF/H_2O (8 mL, 6/2, v/v) in a Teflon reactor (15 mL). Then, the reaction mixture was heated at 110 °C for 3 days. After cooling to room temperature, colorless diamond-shaped crystals of **1** were achieved in a 66% yield based on TIC4R. Element analysis (%) calculated for $C_{134}H_{136}N_{20}O_{34}Zn_4$: C 56.83, H 4.84, N 9.89; found: C 57.11, H 4.72, N 10.09. IR data (KBr, cm^{-1}): 3400 (w), 3130 (w), 2940 (m), 2758 (w), 2670 (w), 1674 (s), 1598 (s), 1532 (m), 1476 (s), 1435 (m), 1364 (s), 1335 (m), 1364 (s), 1230 (m), 1253 (s), 1218 (m), 1147 (w), 1119 (s), 1093 (s), 1059 (m), 1007 (m), 982 (s), 948 (s), 919 (m), 825 (m), 797 (w), 755 (s), 696 (w), 658 (m), 644 (w), 626 (w), 579 (m), 520 (w), 504 (w).

Synthesis of $[Zn_4(TIC4R)_2\cdot(L^2)_2\cdot(OH)_2]\cdot 2HCOO\cdot 4DMF$ (2). **2** was prepared by the similar experimental procedure to that of **1** except that H_2L^1 was replaced by H_2L^2 (7 mg, 0.039 mmol). Yellow diamond-shaped crystals of **2** were achieved in a 68% yield based on TIC4R. Element analysis (%) calculated for $C_{134}H_{138}N_{22}O_{34}Zn_4$: C 56.13, H 4.86, N 10.77; found: C 55.83, H 4.25, N 11.17. IR data (KBr, cm^{-1}): 3440 (m), 3323 (m), 3132 (m), 2970 (m), 2941 (m), 2880 (w), 2759 (w), 2671 (w), 1675 (s), 1604 (s), 1581 (s), 1532 (m), 1476 (s), 1434 (s), 1404 (m), 1382 (s), 1253 (s), 1218 (w), 1147 (m), 1116 (s), 1094 (s), 1060 (m), 1007 (s), 983 (s), 949 (s), 920 (s), 829 (w), 799 (w), 777 (m), 755 (m), 696 (w), 678 (w), 659 (m), 644 (w), 626 (w), 579 (m), 505 (w), 443 (w).

Synthesis of $[Zn_4(TIC4R)_2\cdot(L^3)_2\cdot(OH)_2]\cdot 2HCOO\cdot 3H_2O$ (3). **3** was prepared by the similar

experimental procedure to that of **1** except that H_2L^1 was replaced by H_2L^3 (8 mg, 0.038 mmol) and the ratio of DMF/H_2O was changed to 7/1. Colorless diamond-shaped crystals of **3** were achieved in a 62% yield based on TIC4R. Element analysis (%) calculated for $C_{134}H_{134}N_{22}O_{38}Zn_4$: C 55.08, H 4.62, N 10.55; found: C 55.86, H 4.71, N 10.03. IR data (KBr, cm^{-1}): 3082 (w), 2936 (w), 2759 (w), 1670 (s), 1618 (m), 1557 (s), 1532 (m), 1473 (m), 1436 (w), 1357 (s), 1335 (m), 1299 (w), 1247 (s), 1148 (w), 1114 (m), 1091 (s), 1057 (m), 1005 (m), 977 (s), 943 (s), 917 (s), 822(m), 798 (w), 781 (w),748 (s), 695 (m), 658 (m), 623 (w), 579 (s), 502 (s), 442 (w).

Synthesis of $[Zn_4(TIC4R)_2\cdot(L^4)_2\cdot(OH)_2]\cdot 2HCOO\cdot 3H_2O$ (4). **4** was prepared by the similar experimental procedure to that of **3** except that H_2L^1 was replaced by H_2L^3 (10 mg, 0.046 mmol). Colorless diamond-shaped crystals of **4** were achieved in a 65% yield based on TIC4R. Element analysis (%) calculated for $C_{130}H_{118}N_{16}O_{33}Zn_4$: C 57.96, H 4.41, N 8.32; found: C 57.09, H 4.78, N 8.83. IR data (KBr, cm^{-1}): 3421 (w), 3126 (w), 2941 (w), 2759 (w), 1673 (s), 1614 (s), 1584 (s), 1520 (m), 1475 (s), 1436 (m), 1403 (s), 1385 (s), 1355 (s), 1254 (m), 1148 (w), 1113 (m), 1093 (s), 1060 (m), 1007 (m), 983 (s), 950 (s), 922 (m), 794 (m), 754 (w), 699 (w), 659 (m), 643 (w), 579 (m), 504 (w), 468 (w).

Synthesis of $[Zn_4(TIC4R)_2\cdot(L^5)_2\cdot(OH)_2]\cdot 2HCOO\cdot H_2O$ (5). **5** was prepared by the similar experimental procedure to that of **1** except that H_2L^1 was replaced by H_2L^4 (10 mg, 0.041 mmol) and the ratio of DMF/H_2O was changed to 5/3. Colorless diamond-shaped crystals of **5** were achieved in a 60% yield based on TIC4R. Element analysis (%) calculated for $C_{134}H_{118}N_{16}O_{31}Zn_4$: C 59.39, H 4.39, N 8.27; found: C 58.97, H 4.89, N 8.64. IR data (KBr, cm^{-1}): 3422 (m), 3124 (m), 2941 (m), 2758 (w), 1674 (s), 1609 (s), 1584 (s), 1534 (m), 1475 (s), 1436 (m), 1378 (s), 1255 (s), 1178 (w), 1148 (w), 1117 (s), 1093 (s), 1059 (m), 1006 (m), 982 (s), 948 (s), 919 (m), 860 (w), 839 (w), 799 (w), 773 (s),742 (m), 685 (w), 659 (m), 644(w), 578 (m), 505 (w), 454 (w).

Synthesis of $[Zn_4(TIC4R)_2\cdot(L^6)_2\cdot(OH)_2]\cdot 2HCOO$ (6). **6** was prepared by the similar experimental procedure to that of **3** except that H_2L^3 was replaced by H_2L^5 (10 mg, 0.041 mmol). Colorless diamond-shaped crystals of **6** were achieved in a 42% yield based on TIC4R. Element analysis (%) calculated for $C_{130}H_{112}N_{20}O_{30}Zn_4$: C 57.91, H 4.19, N 10.39; found: C 57.13, H 4.01, N 10.94. IR data (KBr, cm^{-1}): 3432 (w), 3125 (m), 2941 (m), 2765 (w), 1672 (s), 1617 (s), 1593 (s), 1581 (s), 1536 (m), 1475 (s), 1435 (m), 1358 (s), 1301 (m), 1253 (s), 1151 (w), 1116 (s), 1094 (s), 1061 (m), 1009 (m), 984 (s), 950 (s), 923 (m), 843 (w), 781 (m), 755 (w),708 (w), 696 (w), 658 (m), 643 (w), 626(w), 579 (m), 505

(w), 472(w).

Synthesis of $[Zn_4(TIC4R)_2\cdot(L^7)_2\cdot(OH)_2]\cdot 2HCOO\cdot 6DMF$ (7). **7** was prepared by the similar experimental procedure to that of **3** except that H_2L^3 was replaced by H_2L^6 (11 mg, 0.041 mmol). Colorless diamond-shaped crystals of **7** were achieved in a 63% yield based on TIC4R. Element analysis (%) calculated for $C_{156}H_{142}N_{22}O_{36}Zn_4$: C 59.25, H 4.53, N 9.74; found: C 60.01, H 4.12, N 9.96. IR data (KBr, cm^{-1}): 3426 (w), 2941 (m), 2758 (w), 2669 (w), 1674 (s), 1609 (s), 1583 (s), 1559 (m), 1534 (m), 1475 (s), 1436 (m), 1406 (s), 1372 (s), 1301 (m), 1255 (s), 1178 (w), 1148 (w), 1116 (s), 1093 (s), 1059 (m), 1006 (m), 982 (s), 949 (s), 919 (m), 854 (w), 802 (w), 788 (m), 744 (m),708 (w), 696 (w), 659 (m), 644 (m), 578 (m), 529 (w), 504 (w), 426(w).

Synthesis of $[Zn_4(TIC4R)_2\cdot(L^8)_2\cdot(OH)_2]\cdot 2HCOO\cdot 6DMF$ (8). **8** was prepared by the similar experimental procedure to that of **3** except that H_2L^3 was replaced by H_2L^7 (11 mg, 0.041 mmol). Orange diamond-shaped crystals of **8** were achieved in a 58% yield based on TIC4R. Element analysis (%) calculated for $C_{152}H_{158}N_{26}O_{36}Zn_4$: C 57.28, H 5.00, N 11.42; found: C 56.93, H 5.08, N 11.26. IR data (KBr, cm^{-1}): 3413 (w), 3128 (w), 2940 (m), 2757 (w), 2668 (w),1675 (s), 1615 (s), 1583 (s), 1534 (m), 1476 (s), 1436 (m), 1405 (s), 1370 (s), 1304 (m), 1254 (s), 1216 (m), 1148 (w), 1117 (s), 1092 (s), 1059 (m), 1007 (s), 983 (s), 949 (s), 918 (m), 881 (w), 857 (w), 795 (m), 743 (m),707 (w), 696 (w), 659 (m), 643 (m), 578 (m), 504 (w), 425(w).

Synthesis of $[Zn_4(TIC4R)_2\cdot(L^9)_2\cdot(OH)_2]\cdot 2HCOO\cdot 5DMF\cdot 4H_2O$ (9). **9** was prepared by the similar experimental procedure to that of **1** except that H_2L^1 was replaced by H_2L^8 (10 mg, 0.038 mmol) and the reaction temperature was changed to 130 °C. Colorless diamond-shaped crystals of **9** were achieved in a 48% yield based on TIC4R. Element analysis (%) calculated for $C_{161}H_{167}N_{21}O_{39}Zn_4$: C 58.92, H 5.13, N 8.96; found: C 59.05, H 5.75, N 9.88. IR data (KBr, cm^{-1}): 3421 (w), 3127 (w), 2941 (m), 2758 (w), 1674 (s), 1612 (s), 1585 (s), 1558 (m), 1531 (m), 1476 (s), 1436 (m), 1380 (s), 1302 (m), 1248 (s), 1182 (w), 1149 (w), 1115 (m), 1093 (s), 1060 (m), 1007 (s), 983 (s), 949 (s), 920 (m), 838 (m), 780 (s), 748 (w), 696 (w), 658 (m), 643 (w), 625 (w), 578 (m), 504 (w).

Syntheses of Pd@1 and Pd@2. Samples of **Pd@1** and **Pd@2** were synthesized according to the previously reported procedure with a slight modification.[6] HCl (12 mol/L, two drops) and $PdCl_2$ (16.7 mg) were added to water (5 mL), and then the mixture was standed for 2 h until the solid was dissolved. The solution was diluted to produce the H_2PdCl_4 solution (1×10^{-3} M, 100 mL). The activated sample of **1** (150 mg) was dispersed in deionized water (150 mL) and stirred for 0.5 h. The H_2PdCl_4 solution

was added to the resulting suspension with stirring. The mixture was then stirred for 15 h, and the slurry of **[1]$^{+}$·1/2[PdCl$_4$]$^{2-}$** was centrifuged for several times and washed with water. The resulting sample was poured into a solution (5 ml) of 50% hydrazine hydrate (25 mg, 5×10^{-4} mol). The mixture was further stirred for 8 h to yield **Pd@1**. The sample of **Pd@2** was obtained with the same procedure of **Pd@1**. ICP result indicated that *ca.* 0.92 and 1.53% of Pd (mass fraction) were loaded on the samples of **1** and **2**, respectively.

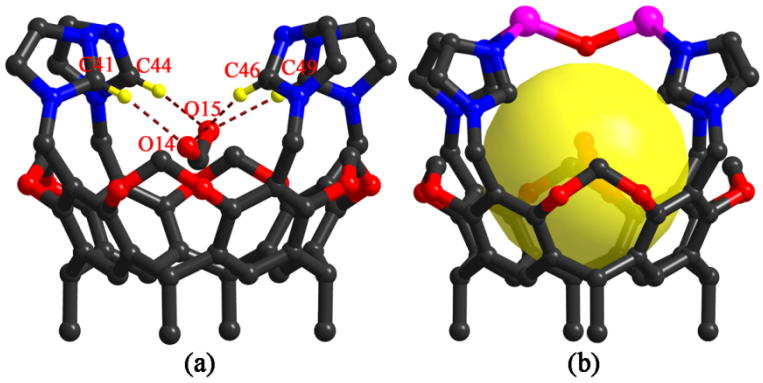

Fig. S1. (a) Hydrogen-bonding interactions between HCOO^{-} and four imidazole linkers of TMC4R. (b) Structure of the bowl-shaped [Zn$_2$(TIC4R)(μ_2-OH(HCOO)]$^{2+}$ unit.

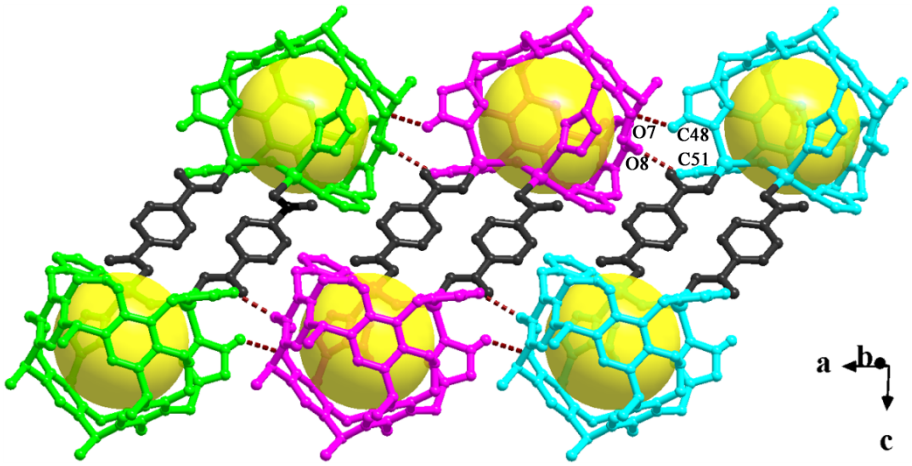

Fig. S2. 1D supramolecular chain linked by hydrogen-bonding interactions (C48H···O7^{ii} = 3.087 Å, C51H···O8^{ii} = 3.228 Å, ^{ii} -1+x, y, z) for **1**.

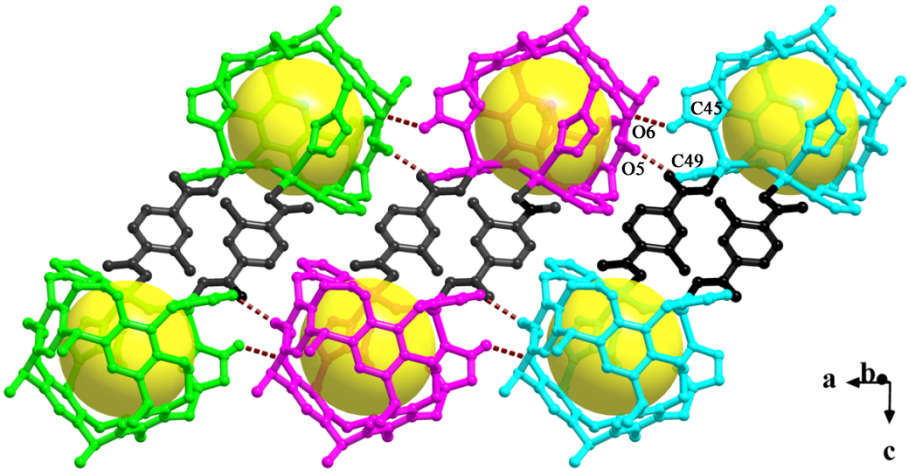

Fig. S3. 1D supramolecular chain linked by hydrogen-bonding interactions (C45H···O6^{ii} = 3.103 Å, C49H···O5^{ii} = 3.287 Å, ^{ii} -x+1, -y, -z+2) for **2**.

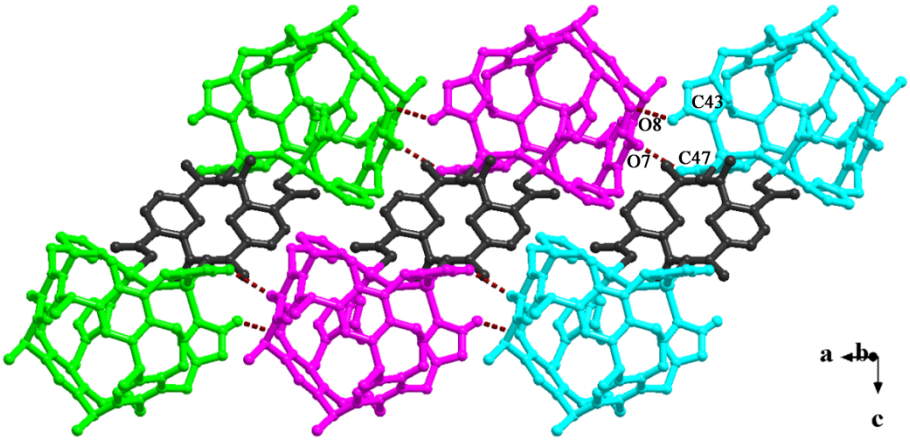

Fig. S4. 1D supramolecular chain linked by hydrogen-bonding interactions (C43H···O8^{ii} = 3.148 Å, C47H···O7^{ii} = 3.338 Å, ^{ii} -x+1, -y+1, -z+1) for **3**.

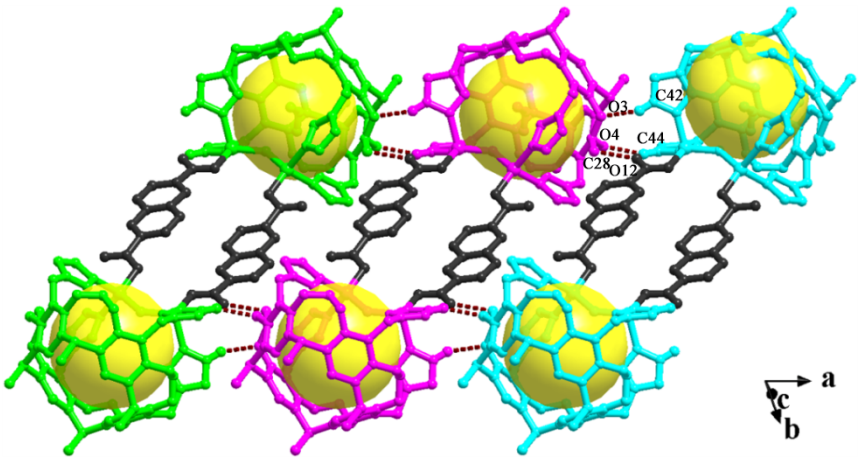

Fig. S5. 1D supramolecular chain linked by hydrogen-bonding interactions (C42H···O3^{ii} = 3.112 Å, C44H···O4^{ii} = 3.302 Å, C28H···O12^{ii} = 3.266 Å, ^{ii} x-1, y, z) for **4**.

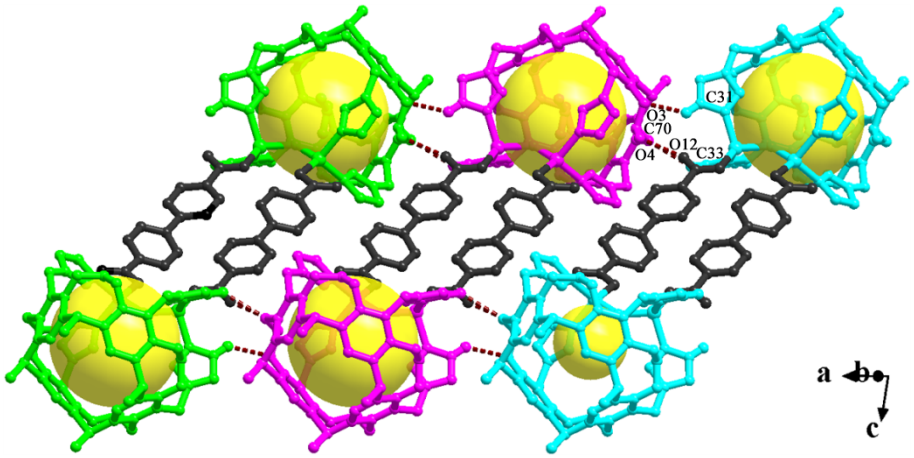

Fig. S6. 1D supramolecular chain linked by hydrogen-bonding interactions (C31H···O3^{i} = 3.074 Å, C33H···O4^{i} = 3.372 Å, C70H···O12^{i} = 3.367 Å, ^{i} x+1, y, z) for **5**.

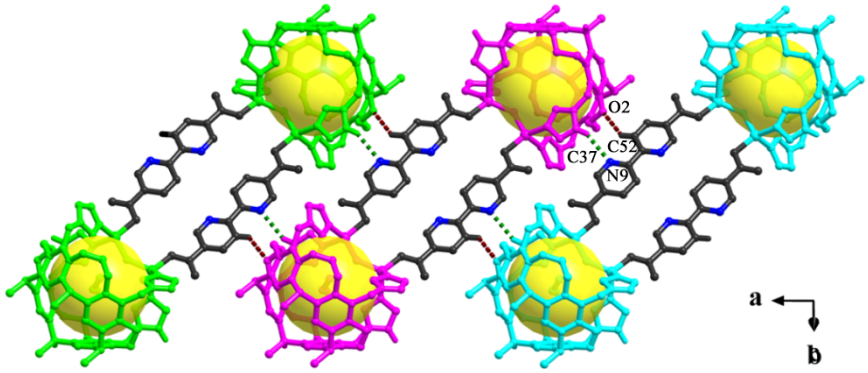

(a)

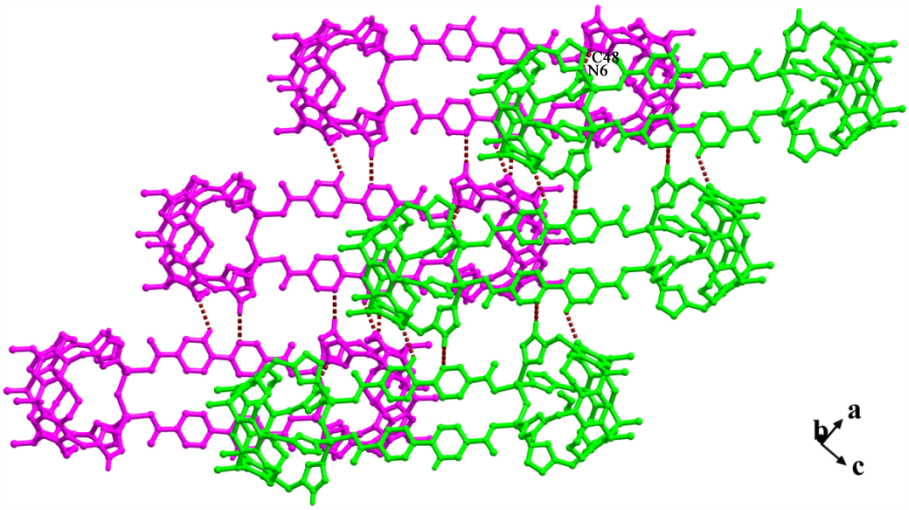

(b)

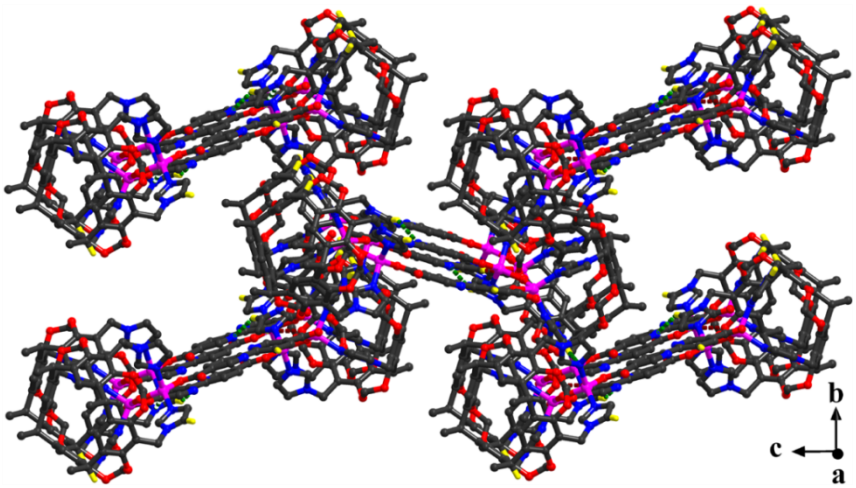

(c)

Fig. S7. (a) 1D supramolecular chain linked by hydrogen-bonding interactions (C37H···N9^{ii} = 3.328 Å, C52H···O2^{ii} = 3.346 Å, ^{ii} x+1, y, z) for **6**. (b) 2D supramolecular layer formed by hydrogen bonds (C48H···N6^{iii} = 3.274 Å, ^{iii} -x+1/2, y+1/2, -z+1/2) for **6**. (c) 3D supramolecular structure formed by hydrogen bond interactions (C37H···N9^{ii} = 3.328 Å, C52H···O2^{ii} = 3.346 Å, C48H···N6^{iii} = 3.274 Å, ^{ii} x+1, y, z, ^{iii} -x+1/2, y+1/2, -z+1/2) for **6**.

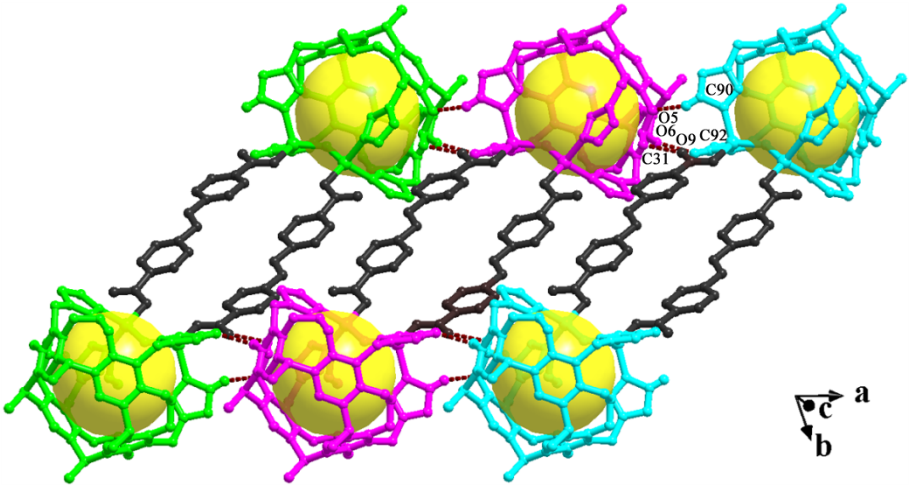

Fig. S8. 1D supramolecular chain linked by hydrogen-bonding interactions (C90H···O5^{ii} = 3.093 Å, C92H···O6^{ii} = 3.202 Å, C31H···O9^{ii} = 3.202 Å, ^{ii} x+1, y, z) for **7**.

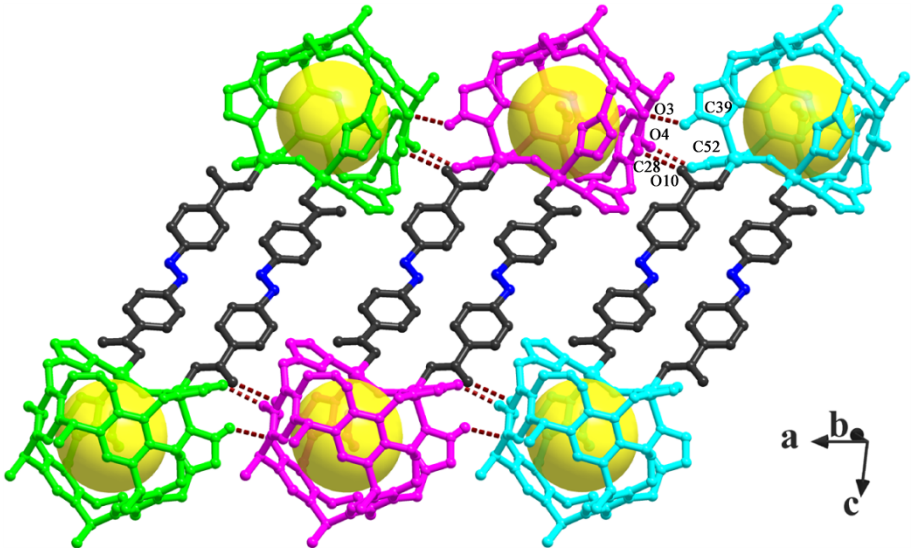

Fig. S9. 1D supramolecular chain linked by hydrogen-bonding interactions (C52H···O4^{ii} = 3.181 Å, C39H···O3^{ii} = 3.079 Å, C28H···O10^{ii} = 3.390 Å, ^{ii} -1+x, y, z) for **8**.

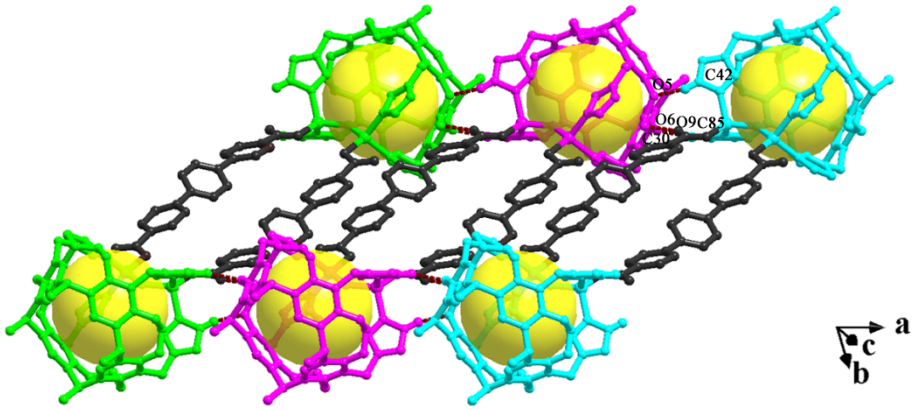

Fig. S10. 1D supramolecular chain linked by hydrogen-bonding interactions (C30H···O9^{ii} = 3.323 Å, C42H···O5^{iii} = 3.094 Å, C85H···O6^{iii} = 3.251 Å, ^{ii} -x, -y-1, -z+1, -x, -y-1, -z+1) for **9**.

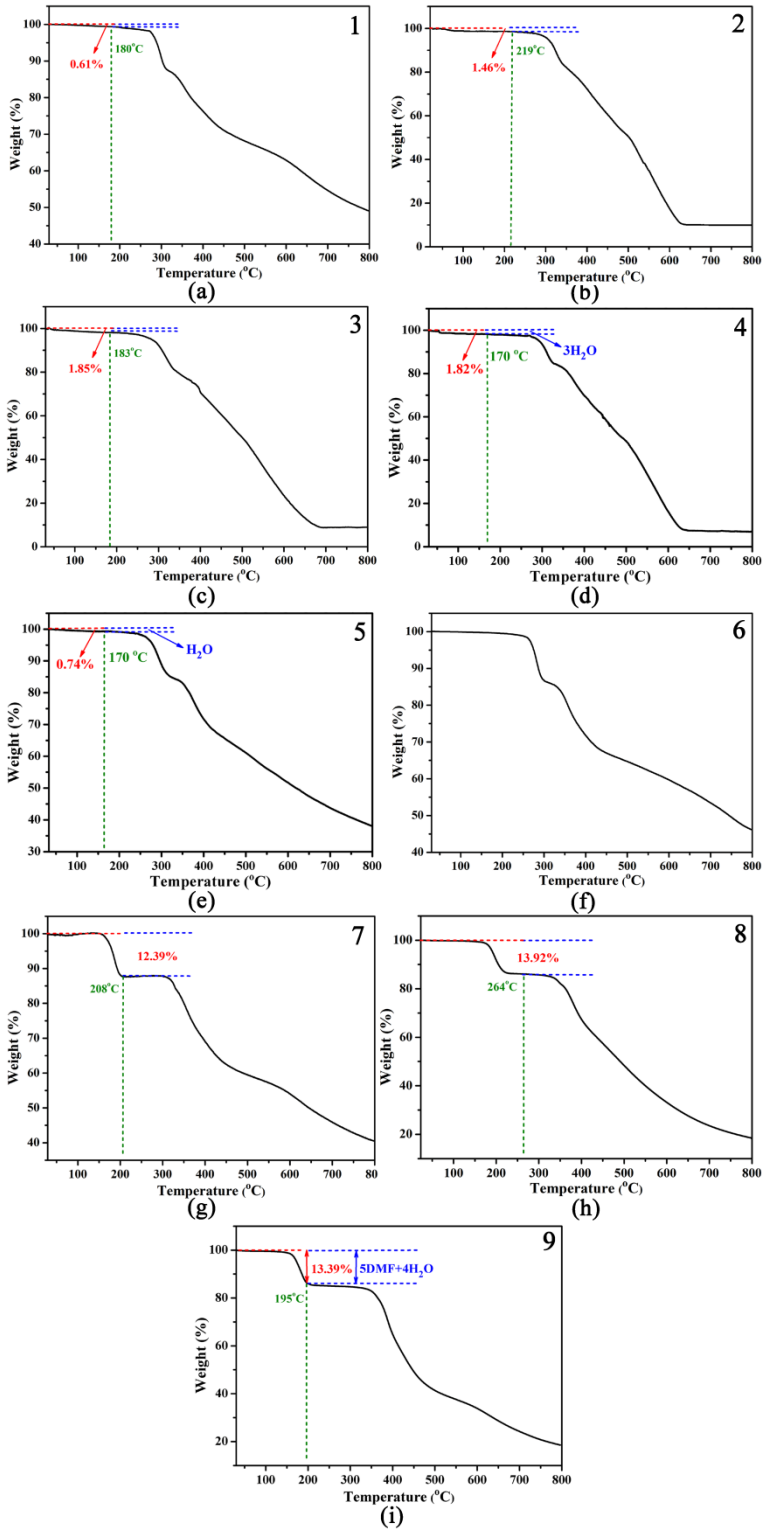

Fig. S11. Thermogravimetric curves of **1-9**. The weight losses of 0.61% (calcd. 10.32%), 1.46% (calcd. 10.21%), 1.85% (calcd. 10.01%), 1.82% (calcd. 2.00%), 0.74% (calcd. 0.66%), 12.39% (calcd. 13.87%), 13.92% (calcd. 13.76%) and 13.39% (calcd. 13.31%) corresponded to the solvent removal of **1-5** and **7-9**, respectively. For compounds **1-3**, their actual weight loss is lower than the calculated one. It can be attributed to the loss of solvent molecules during the storage.

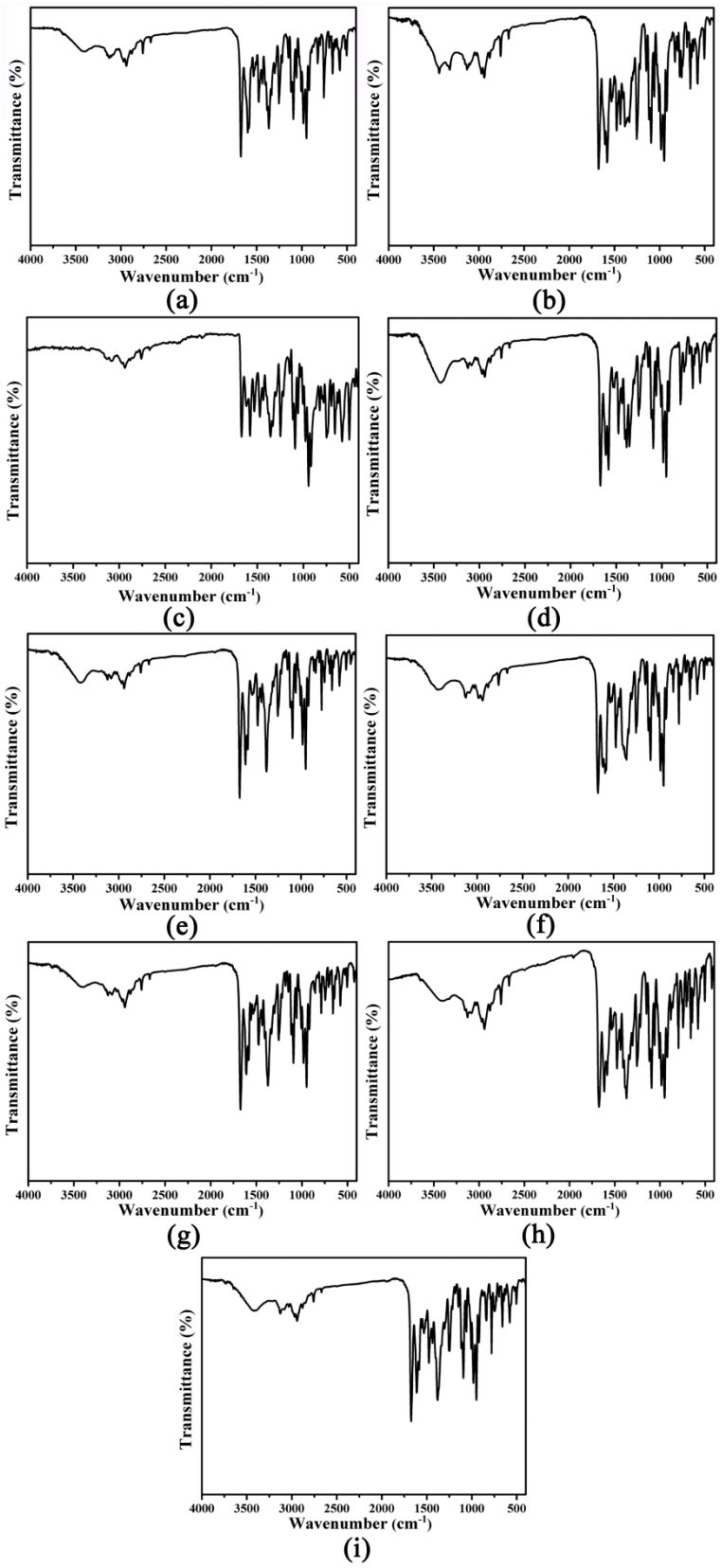

Fig. S12. FT-IR spectra of (a)-(i) for **1-9**, respectively.

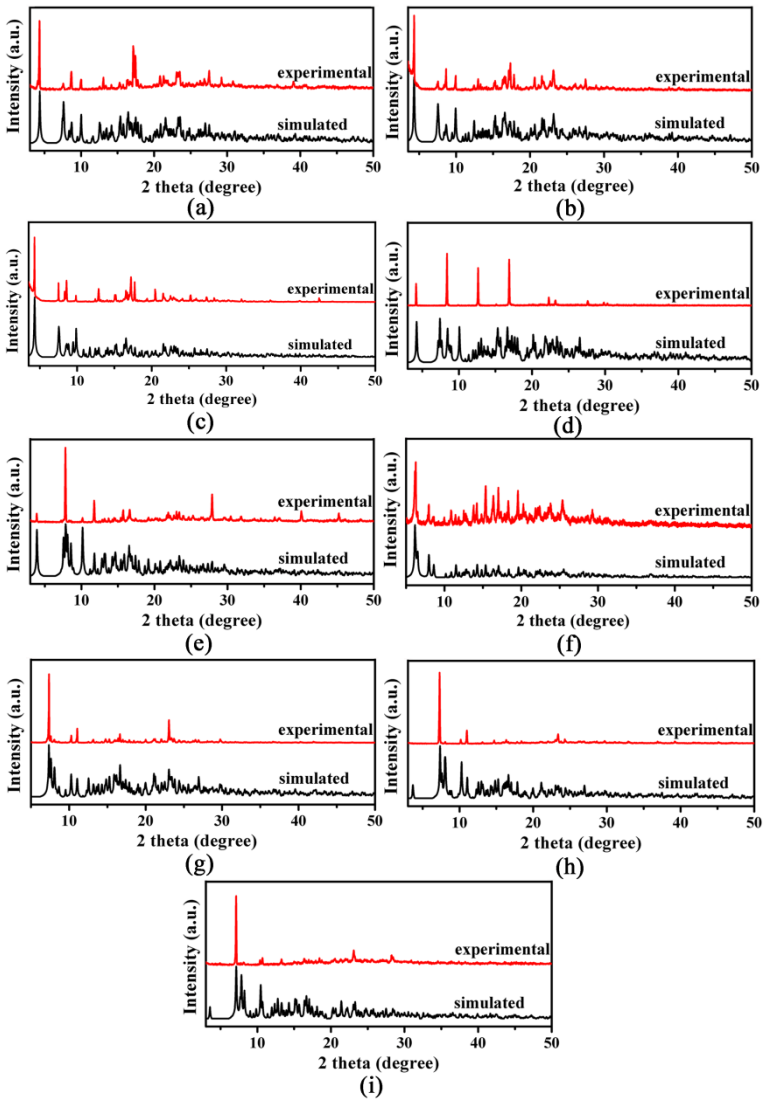

Fig. S13. PXRD patterns (a)-(i) for **1-9**, respectively.

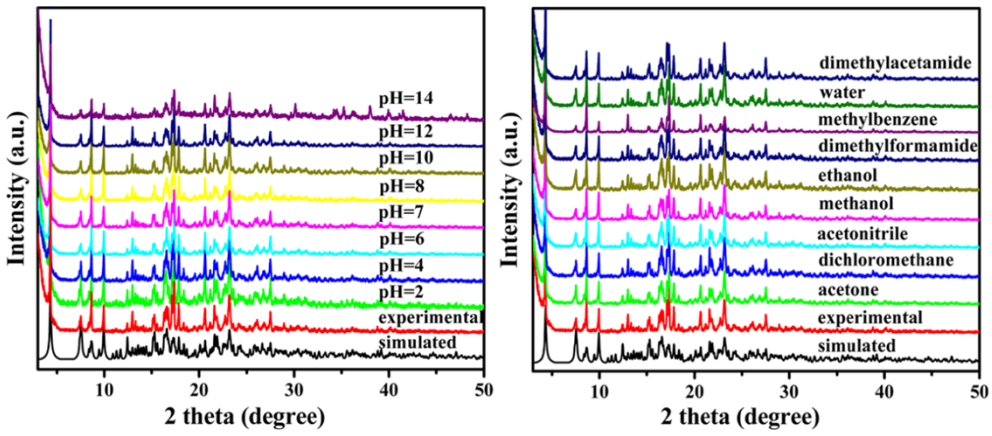

(a) (b)

Fig. S14. PXRD patterns of **2** in aqueous solutions (pH = 2-14) (a) and organic solvents (b).

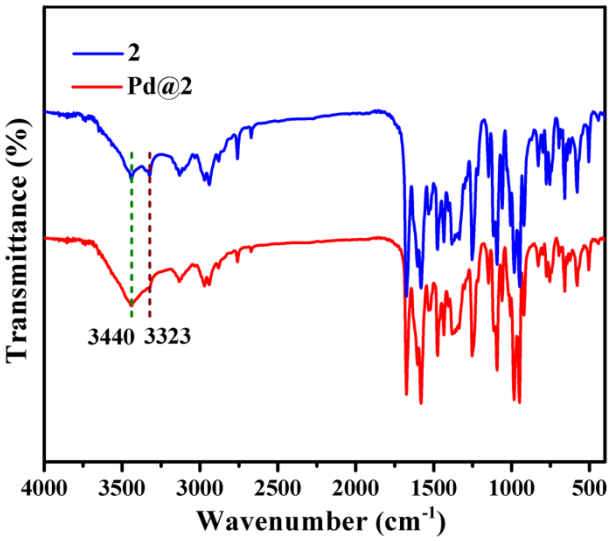

Fig. S15. FT-IR spectra of **2** and **Pd@2**.

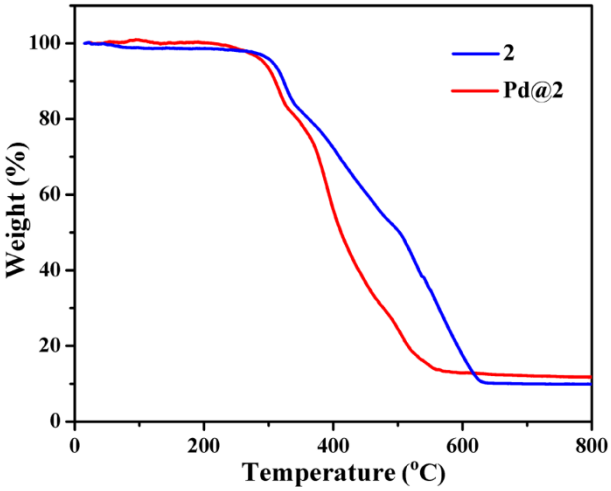

Fig. S16. Thermogravimetric curve of **2** and **Pd@2**.

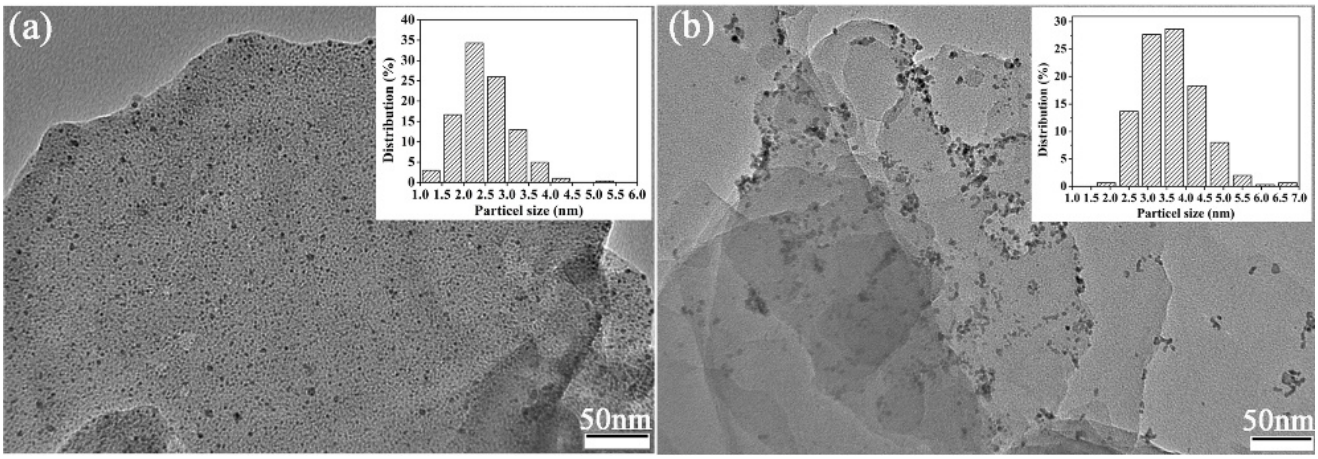

Fig. S17. TEM image of **Pd@2** (a) and **Pd@1** (b) before catalysis.

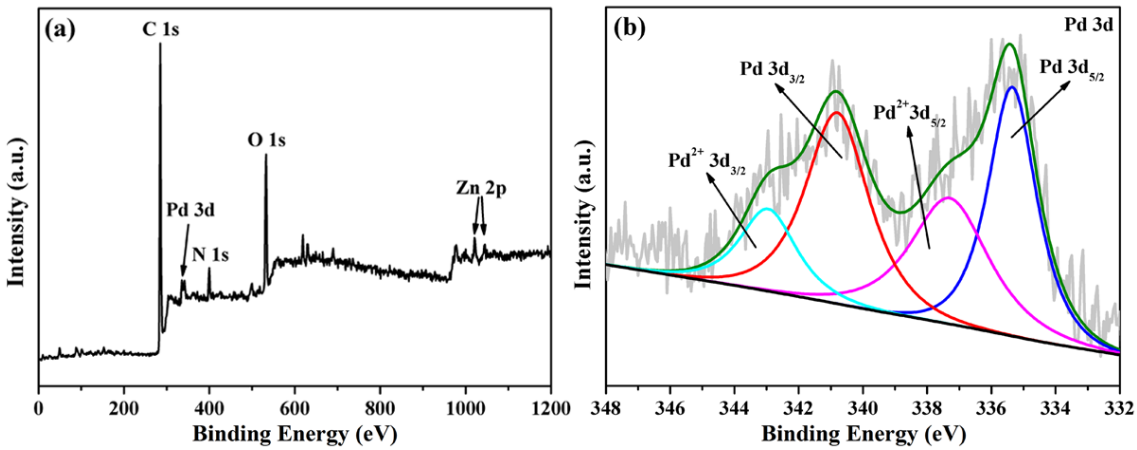

Fig. S18. XPS wide-scan spectrum (a) and fine Pd 3d spectrum (b) of **Pd@2**.

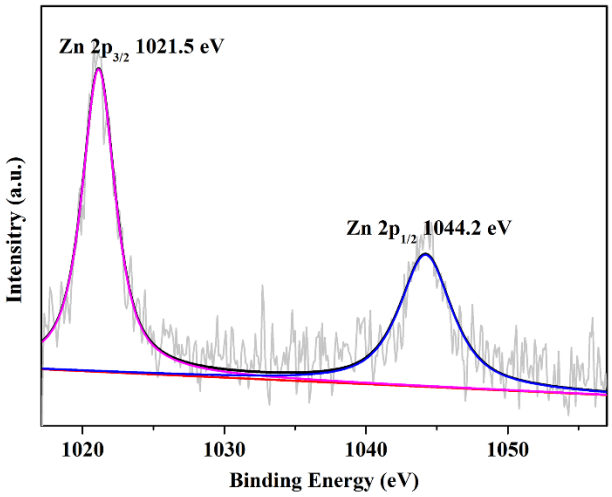

Fig. S19. XPS survey scans of Zn 2p.

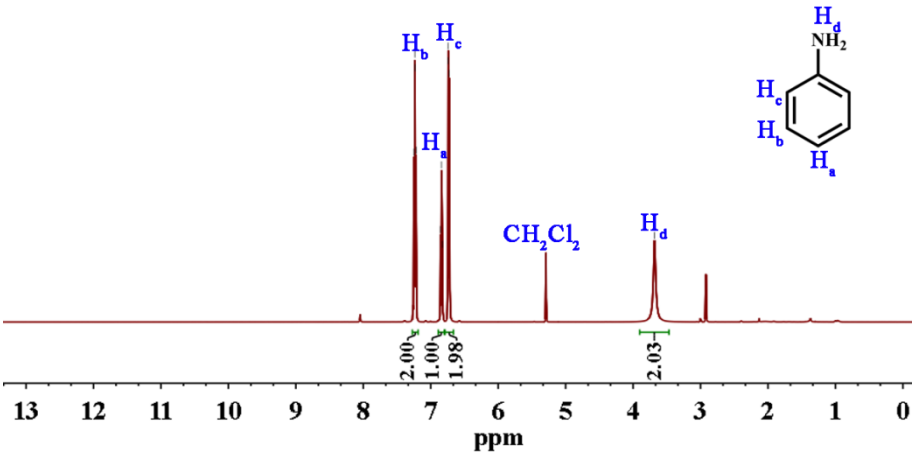

Fig. S20. ^{1}H NMR spectra of the crude product from the tandem reaction of the NH_3BH_3 dehydrogenation and nitrobenzene hydrogenation. To gain clear ^{1}H NMR spectrum, amounts of the

reactant and catalyst were increased five times (nitrobenzene: 0.5 mmol, catalyst: 50 mg, NH_3BH_3: 1.5 mmol, water: 25 mL, time: 10 min, room temperature). (500 MHz, $CDCl_3$) δ = 7.22 (t, *J* = 7.6 Hz, 2H), 6.84 (t, *J* = 7.4 Hz, 1H), 6.73 (d, *J* = 7.7 Hz, 2H), 2.03(s, 2H).

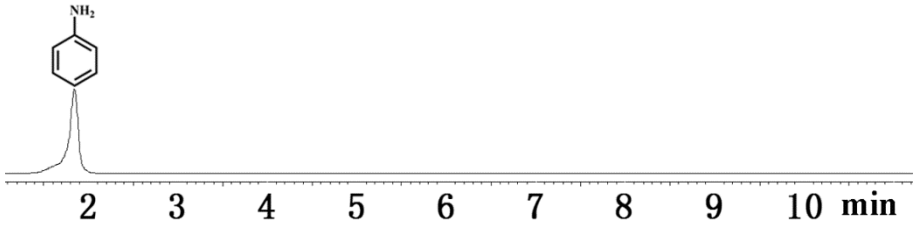

(a)

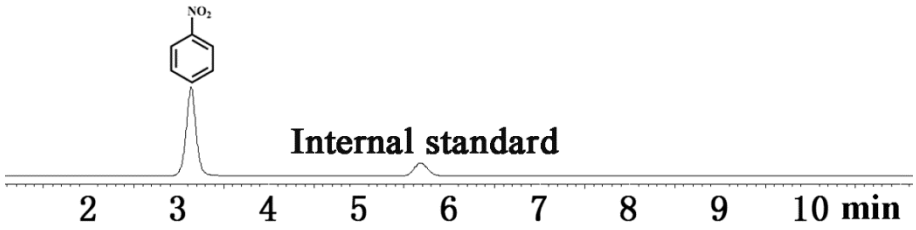

(b)

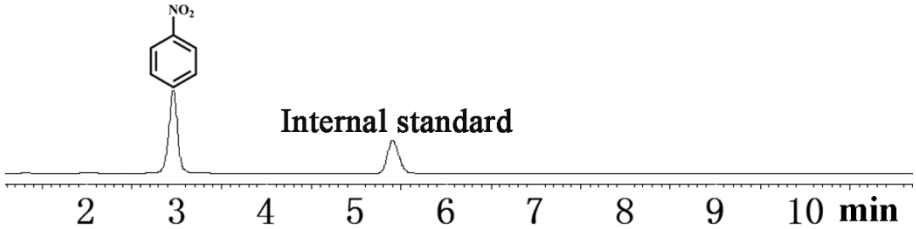

(c)

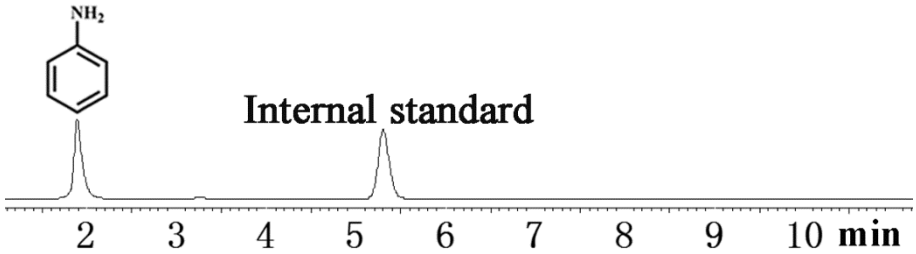

(d)

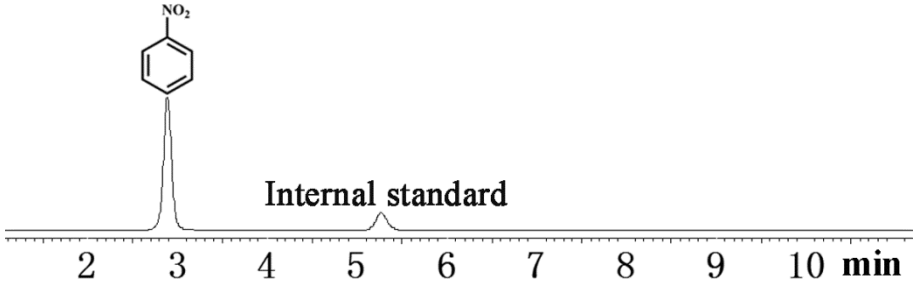

(e)

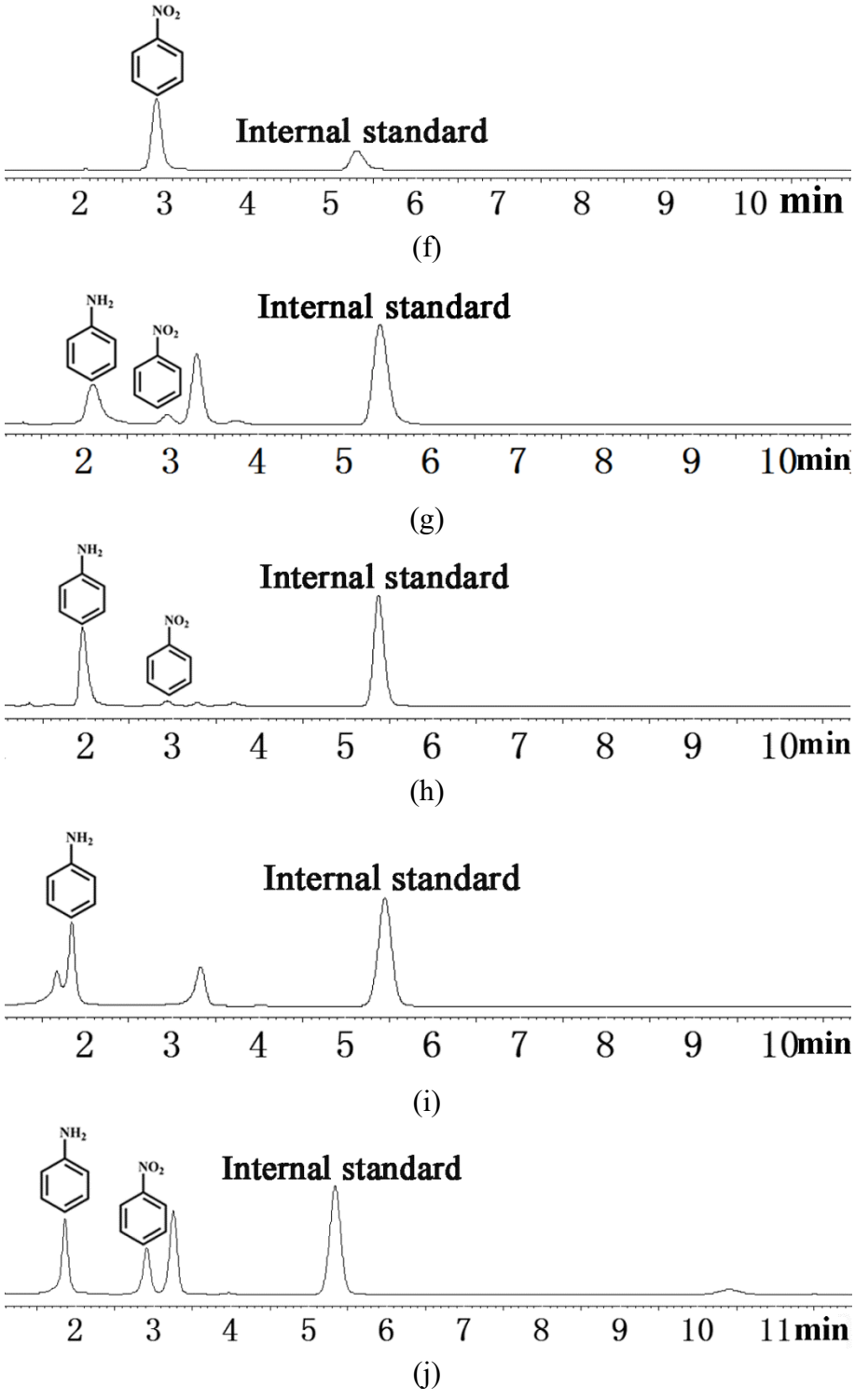

Fig. S21. HPLC spectra for nitrobenzene hydrogenation for 10 min at room temperature: (a) the standard aniline sample, (b) in water without catalyst and NH_3BH_3 (0.3 mmol) as reductant, (c) in water with **2** (10 mg) and NH_3BH_3 (0.3 mmol) as reductant, (d) in water with **Pd@2** (10 mg) and NH_3BH_3 (0.3 mmol) as reductant, (e) in water with **Pd@2** (10 mg) and without NH_3BH_3, (f) in water with **Pd@2** (10 mg) at 1 atm H_2, (g) in methanol with **Pd@2** (10 mg) and NH_3BH_3 (0.3 mmol) as reductant, (h) in methanol and water (v/v = 2:3) with **Pd@2** (10 mg) and NH_3BH_3 (0.3 mmol) as

reductant, (i) in methanol and water (v/v = 4:1) with **Pd@2** (10 mg) and NH_3BH_3 (0.3 mmol) as reductant , (j) in water with **Pd@1** (10 mg) and NH_3BH_3 (0.3 mmol) as reductant.

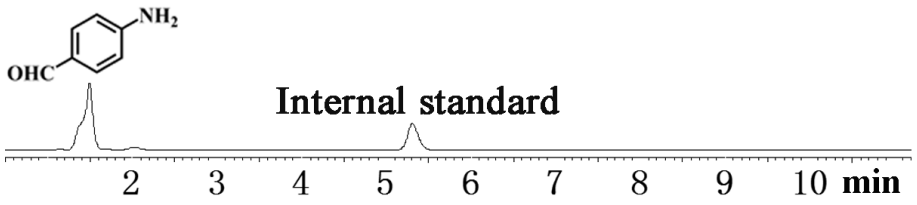

(a)

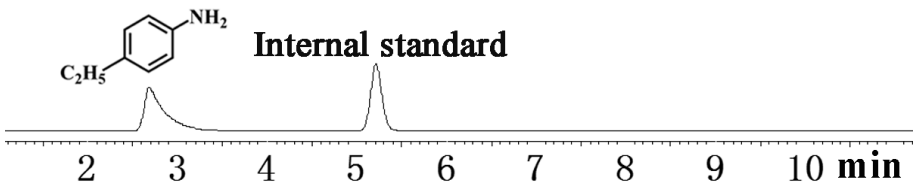

(b)

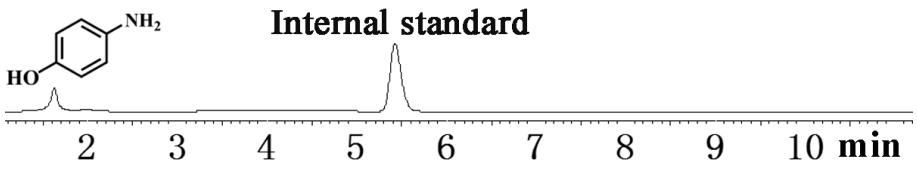

(c)

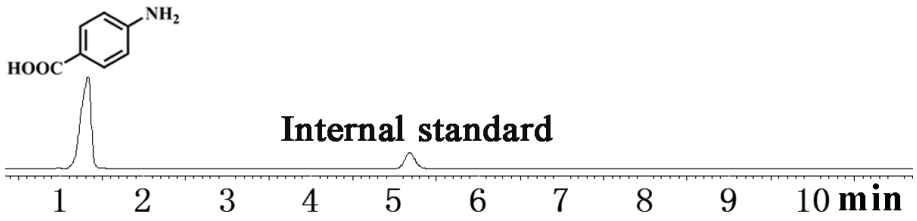

(d)

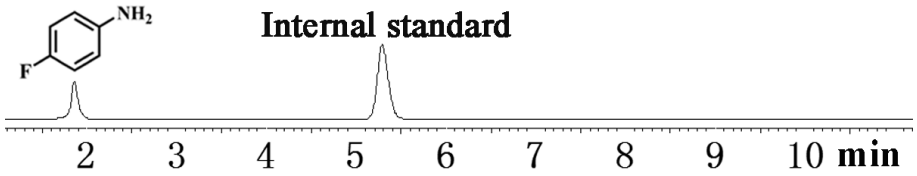

(e)

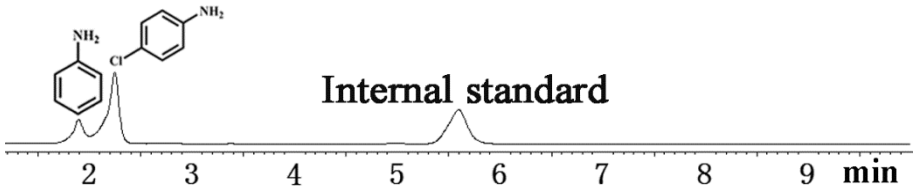

(f)

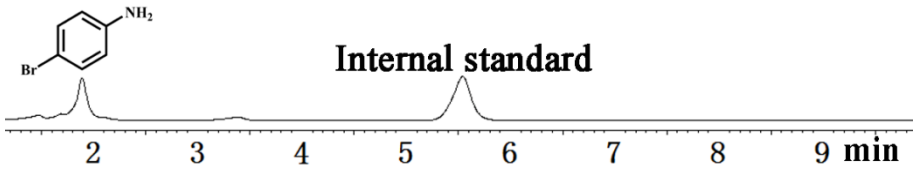
NH2
Br
Internal standard
2 3 4 5 6 7 8 9 min

(g)

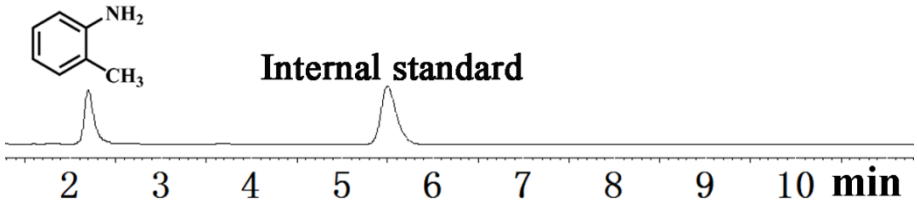
NH2
CH3
Internal standard
2 3 4 5 6 7 8 9 10 min

(h)

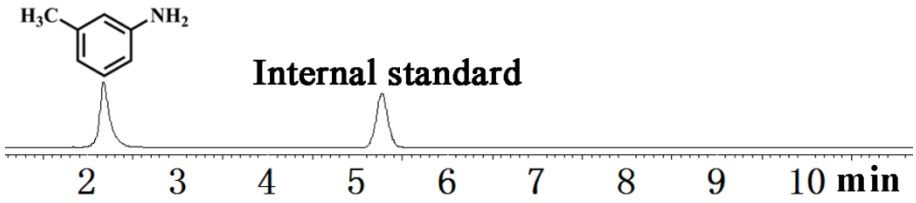
H3C
NH2
Internal standard
2 3 4 5 6 7 8 9 10 min

(i)

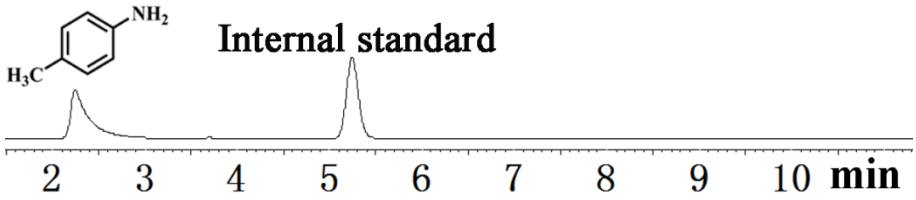
NH2
H3C
Internal standard
2 3 4 5 6 7 8 9 10 min

(g)

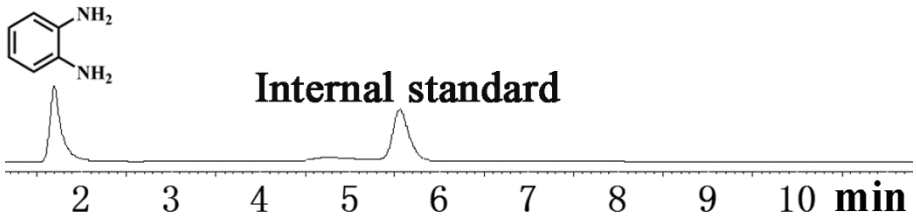
NH2
NH2
Internal standard
2 3 4 5 6 7 8 9 10 min

(k)

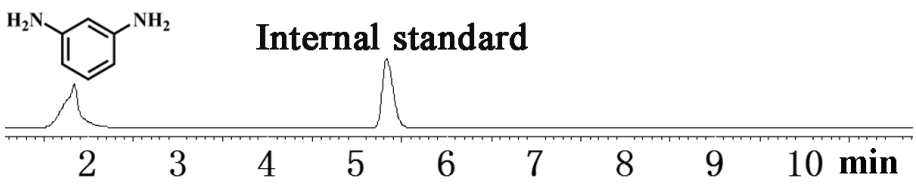
H2N
NH2
Internal standard
2 3 4 5 6 7 8 9 10 min

(l)

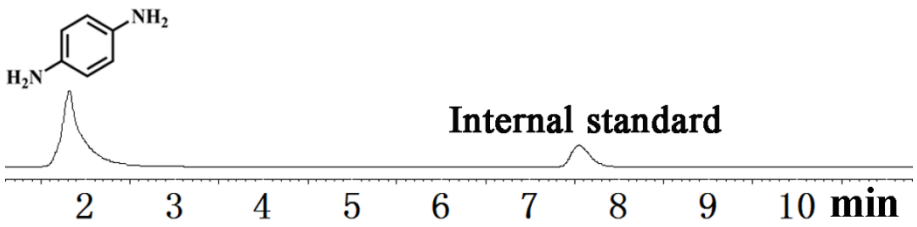

(m)

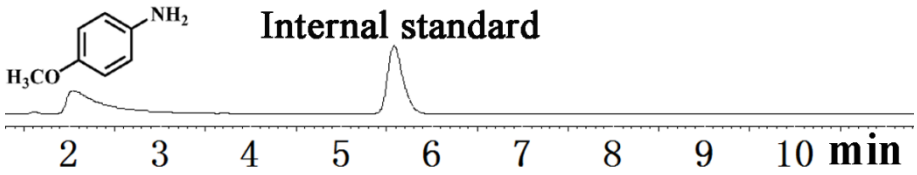

(n)

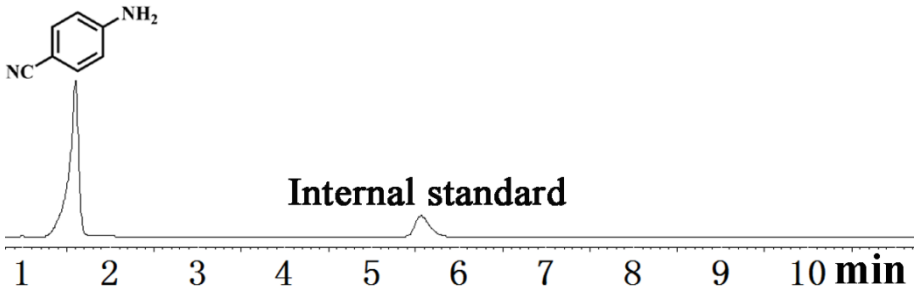

(o)

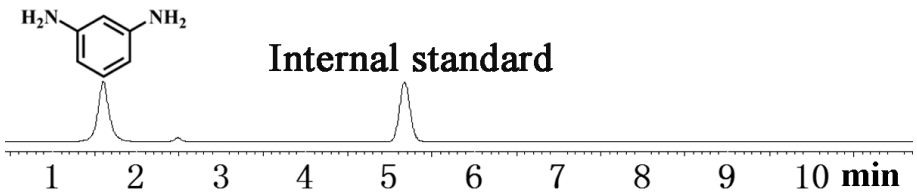

(p)

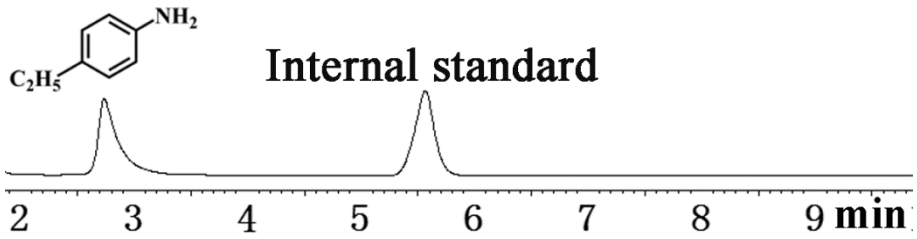

(q)

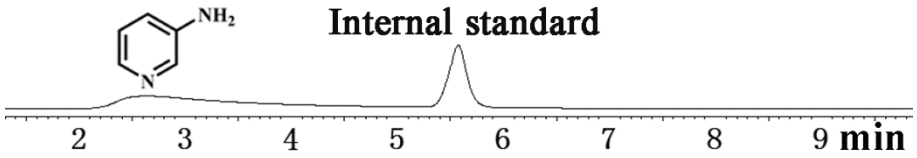

(r)

Fig. S22. HPLC spectra for the NH_3BH_3 dehydrogenation and nitroarene hydrogenation with **Pd@2**

at room temperature: (a) 4-nitrobenzaldehyde, (b) 4-nitroethylbenzene, (c) 4-nitrophenol, (d) 4-nitrobenzoic acid, (e) 4-fluoronitrobenzene, (f) 4-nitrochlorobenzene, (g) 4-bromonitrobenzene, (h) 2-nitrotoluene, (i) 3-nitrotoluene, (j) 4-nitrotoluene, (k) 2-nitroaniline, (l) 3-nitroaniline, (m) 4-nitroanilie, (n) 4-nitroanisole, (o) 4-nitrobenzonitrile, (p) 1,3-dinitrobenzene, (q) 4-nitroethynylbenzene, (r) 3-nitropyridine. The catalytic product was dealed with CH_3OH.

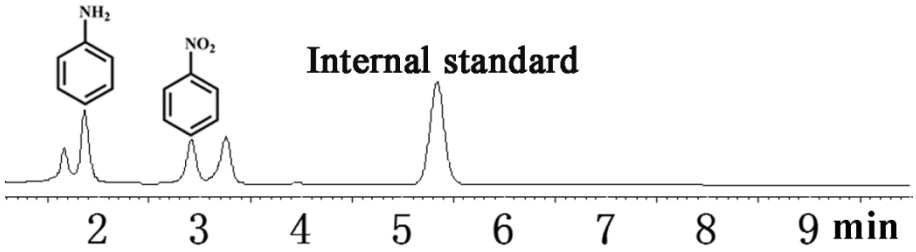

(a)

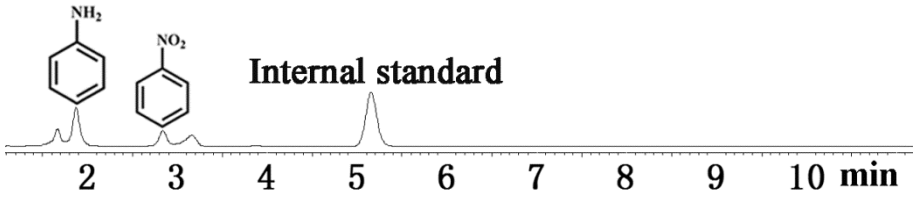

(b)

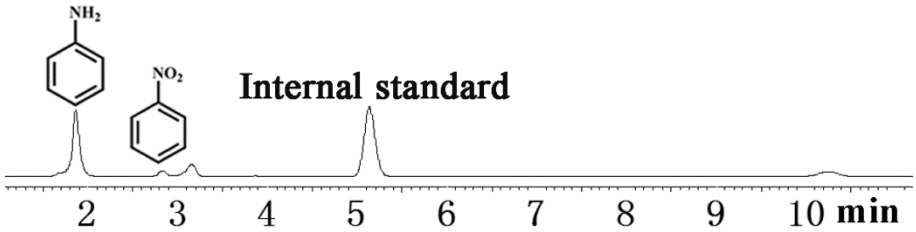

(c)

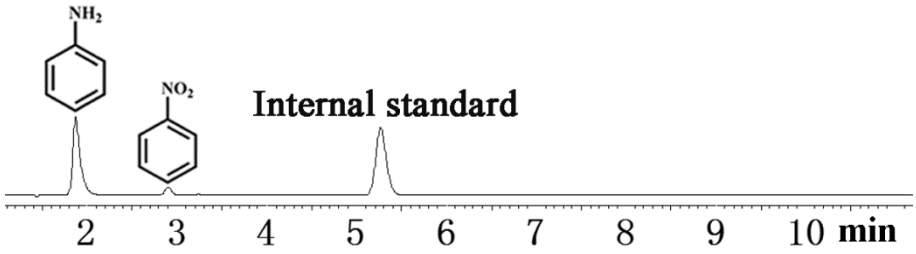

(d)

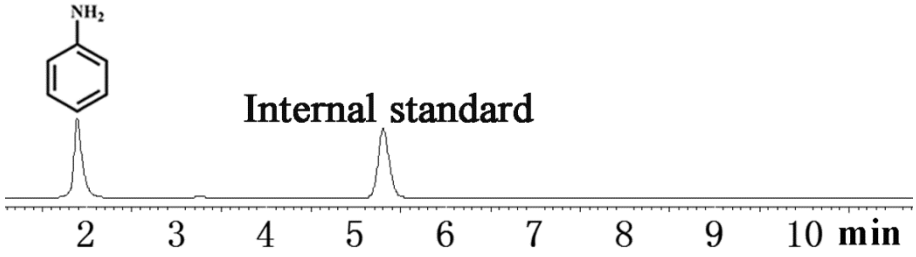

(e)

Fig. S23. HPLC Spectra of the NH_3BH_3 dehydrogenation and nitrobenzene hydrogenation at room temperature: (a) 10 mg **Pd@2** as catalyst for 2 min, (b) 10 mg **Pd@2** as catalyst for 4 min, (c) 10 mg **Pd@2** as catalyst for 6 min, (d) 10 mg **Pd@2** as catalyst for 8 min and (e) 10 mg **Pd@2** as catalyst for 10 min.

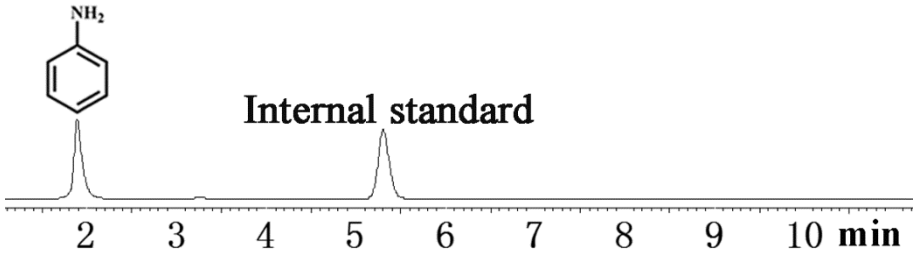

(a)

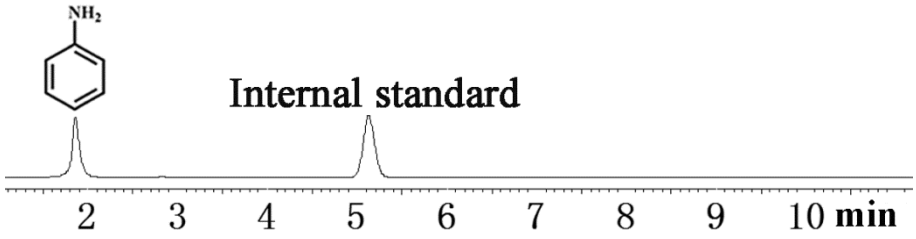

(b)

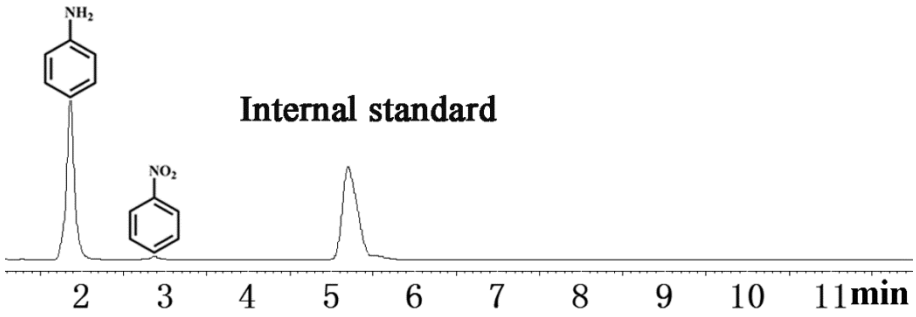

(c)

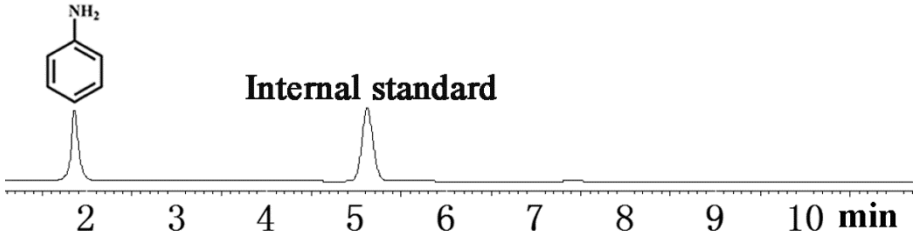

(d)

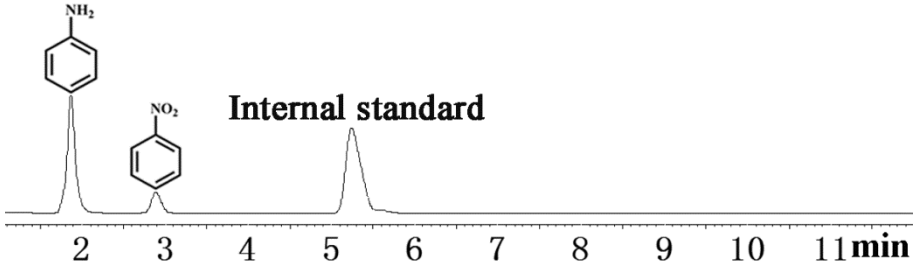

(e)

Fig. S24. HPLC spectra of tandem reaction for the recycled experiments with **Pd@2**: (a) the first cycle, (b) the second cycle, (c) the third cycle, (d) the fourth cycle and (e) the fifth cycle.

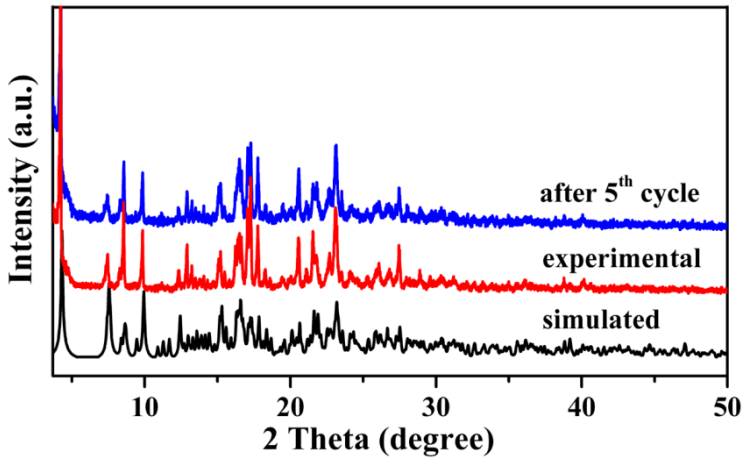

Fig. S25. PXRD patterns: the simulated **2** (black), the experimental **2** (red) and that after five cycles with **Pd@2** (blue).

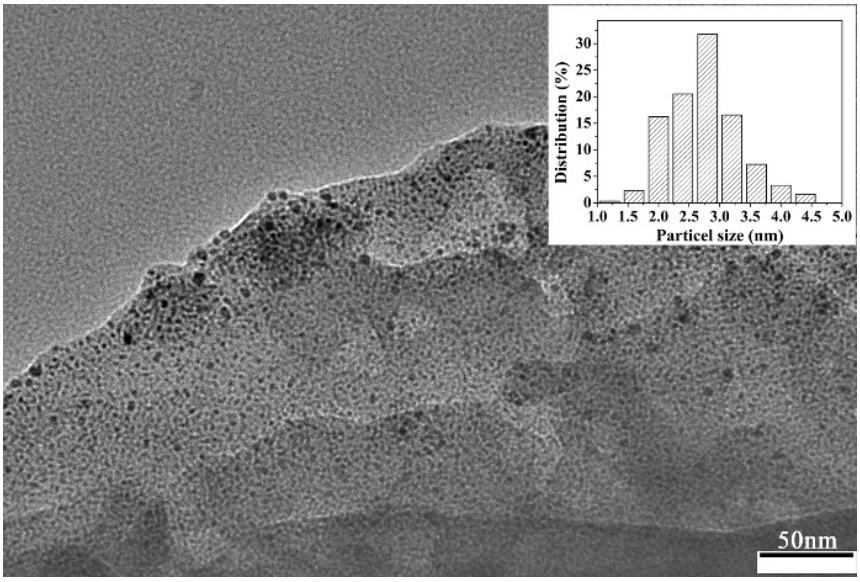

Fig. S26. TEM image of **Pd@2** after the recycling tests.

Table S1. Crystallographic data for **1-8**.

Compound	**1**	**2**	**3**
Formula	$C_{134}H_{136}N_{20}O_{34}Zn_4$	$C_{134}H_{138}N_{22}O_{34}Zn_4$	$C_{134}H_{134}N_{22}O_{38}Zn_4$
Mr	2832.10	2862.29	2922.09
Crystal system	Triclinic	Triclinic	Triclinic
Space group	*P*-1	*P*-1	*P-1*
a(Å)	12.6235(7)	12.6328(5)	12.6584(5)
b(Å)	13.2691(7)	13.2282(5)	13.2356(5)
c(Å)	20.9836(12)	21.1070(8)	21.2394(9)
α(°)	75.250(5)	75.676(3)	75.538(4)
β(°)	84.917(5)	86.550(3)	86.914(3)
γ(°)	66.924(5)	67.967(4)	67.873(4)
V(Å^3)	3126.8(3)	3165.8(2)	3188.7(2)
Z	1	1	1
T(K)	298	298	298
D_{calc}(g cm^{-3})	1.504	1.501	1.521
F(000)	1472	1488	1514
R_{int}	0.0372	0.0274	0.0319
GOF on F^2	1.056	1.060	1.044
$R_1{}^a$ [I>2σ(I)]	0.0548	0.0505	0.0784
$wR_2{}^b$ (all data)	0.1423	0.1473	0.2508

Compound	**4**	**5**	**6**
Formula	$C_{130}H_{118}N_{16}O_{33}Zn_4$	$C_{134}H_{118}N_{16}O_{31}Zn_4$	$C_{130}H_{112}N_{20}O_{30}Zn_4$
Mr	2693.88	2709.92	2695.87
Crystal system	Triclinic	Triclinic	Monoclinic
Space group	*P*-1	*P*-1	*P21*/*n*
a(Å)	12.7117(5)	12.6930(6)	15.9426(8)
b(Å)	13.3519(9)	13.1976(8)	15.3658(7)
c(Å)	21.3024(16)	22.9243(15)	28.7074(15)
α(°)	78.814(6)	81.532(5)	90
β(°)	85.301(5)	80.885(5)	91.722(4)
γ(°)	69.705(5)	67.896(5)	90
V(Å^3)	3326.3(4)	3496.9(4)	7029.3(6)
Z	1	1	2
T(K)	298	298	298
D_{calc} (g cm^{-3})	1.345	1.287	1.274
F(000)	1394	1402	2784
R_{int}	0.0302	0.0265	0.0301
GOF on F^2	1.012	1.044	1.046
$R_1{}^a$ [I>2σ(I)]	0.0492	0.0466	0.0514
$wR_2{}^b$ (all data)	0.1206	0.1213	0.1495
Compound	**7**	**8**	**9**
Formula	$C_{156}H_{142}N_{22}O_{36}Zn_4$	$C_{152}H_{158}N_{26}O_{36}Zn_4$	$C_{161}H_{167}N_{21}O_{39}Zn_4$
Mr	3162.39	3186.51	3281.63
Crystal system	Triclinic	Triclinic	Triclinic
Space group	*P*-1	*P*-1	*P*-1
a(Å)	12.5964(4)	12.5628(5)	12.6324(5)
b(Å)	13.2279(6)	13.2187(5)	13.1859(5)
c(Å)	24.2610(12)	24.0978(9)	25.2091(10)
α(°)	86.566(4)	86.376(3)	89.431(3)
β(°)	81.593(3)	81.813(3)	79.959(4)
γ(°)	68.079(4)	67.430(4)	68.233(4)
V(Å^3)	3709.8(3)	3657.5(3)	3833.1(3)
Z	1	1	1
T(K)	298	298	298
D_{calc} (g cm^{-3})	1.416	1.447	1.422

F(000)	1640	1660	1712
R_{int}	0.0413	0.0312	0.0306
GOF on F^2	1.041	1.027	0.990
$R_1{}^a$ [I>2σ(I)]	0.0649	0.0652	0.0451
$wR_2{}^b$ (all data)	0.1921	0.1816	0.1064

$^aR_1 = \Sigma||F_o| - |F_c||/\Sigma|F_o|$. $^bwR_2 = \{\Sigma[w(F_o^2-F_c^2)^2]/\Sigma w(F_o^2)^2]\}^{1/2}$

Table S2. Selected bond lengths [Å] and angles [deg] for **1**.

1			
Zn(1)-O(9)	1.919(2)	Zn(1)-O(13)^i	1.935(2)
Zn(1)-N(8)	2.025(3)	Zn(1)-N(6)	2.040(3)
Zn(2)-O(9)	1.909(3)	Zn(2)-O(11)	1.934(2)
Zn(2)-N(2)	2.030(3)	Zn(2)-N(4)	2.044(3)
O(9)-Zn(1)-O(13)^i	109.93(11)	O(9)-Zn(1)-N(8)	109.87(12)
O(13)^i-Zn(1)-N(8)	112.53(12)	O(9)-Zn(1)-N(6)	104.80(12)
O(13)^i-Zn(1)-N(6)	120.64(12)	N(8)-Zn(1)-N(6)	98.19(12)
O(9)-Zn(2)-O(11)	109.65(12)	O(9)-Zn(2)-N(2)	106.49(12)
O(11)-Zn(2)-N(2)	118.60(12)	O(9)-Zn(2)-N(4)	110.29(12)
O(11)-Zn(2)-N(4)	113.39(12)	N(2)-Zn(2)-N(4)	97.70(12)

Symmetry code: ^{i} -x+1,-y,-z+2.

Table S3. Selected bond lengths [Å] and angles [deg] for **2**.

2			
Zn(1)-O(13)	1.916(3)	Zn(1)-O(9)	1.931(3)
Zn(1)-N(6)	2.029(3)	Zn(1)-N(7)	2.036(3)

Zn(2)-O(13)	1.905(3)	Zn(2)-O(12)^{i}	1.937(3)
Zn(2)-N(4)	2.027(3)	Zn(2)-N(2)	2.040(3)
O(13)-Zn(1)-O(9)	110.28(11)	O(13)-Zn(1)-N(6)	109.89(13)
O(9)-Zn(1)-N(6)	112.66(13)	O(13)-Zn(1)-N(7)	104.77(13)
O(9)-Zn(1)-N(7)	120.51(13)	N(6)-Zn(1)-N(7)	97.78(13)
O(13)-Zn(2)-O(12)^{i}	110.45(12)	O(13)-Zn(2)-N(4)	106.58(13)
O(12)^{i}-Zn(2)-N(4)	117.97(13)	O(13)-Zn(2)-N(2)	110.21(13)
O(12)^{i}-Zn(2)-N(2)	113.48(12)	N(4)-Zn(2)-N(2)	97.30(14)

Symmetry code: ^{i} -x-1,-y+1,-z.

Table S4. Selected bond lengths [Å] and angles [deg] for **3**.

3			
Zn(1)-O(11)	1.914(4)	Zn(1)-O(14)^{i}	1.990(5)
Zn(1)-N(4)	2.028(5)	Zn(1)-N(6)	2.024(3)
Zn(2)-O(11)	1.904(4)	Zn(2)-O(12)	1.931(4)
Zn(2)-N(2)	2.035(5)	Zn(2)-N(8)	2.028(4)
O(11)-Zn(1)-O(14)^{i}	112.64(19)	O(11)-Zn(1)-N(4)	104.77(18)
O(14)^{i}-Zn(1)-N(4)	121.20(2)	O(11)-Zn(1)-N(6)	109.83(18)
O(14)^{i}-Zn(1)-N(6)	109.40(2)	N(6)-Zn(1)-N(4)	97.71(19)
O(11)-Zn(2)-O(12)	112.25(19)	O(11)-Zn(2)-N(2)	109.11(19)
O(13)-Zn(2)-N(8)	105.94(18)	O(12)-Zn(2)-N(2)	113.82(19)
O(12)-Zn(2)-N(8)	116.55(19)	N(8)-Zn(2)-N(2)	98.01(19)

Symmetry code: ^{i} –x+2, -y, -z+2.

Table S5. Selected bond lengths [Å] and angles [deg] for **4**.

4			
Zn(1)-O(11)	1.903(3)	Zn(1)-O(14)^{i}	1.917(2)
Zn(1)-N(7)	2.015(3)	Zn(1)-N(9)	2.036(3)
Zn(2)-O(11)	1.913(2)	Zn(2)-O(13)	1.939(2)
Zn(2)-N(3)	2.023(3)	Zn(2)-N(2)	2.040(3)
O(11)-Zn(1)-O(14)^{i}	108.24(11)	O(11)-Zn(1)-N(7)	107.82(13)
O(14)^{i}-Zn(1)-N(7)	119.95(11)	O(11)-Zn(1)-N(9)	108.88(12)
O(14)^{i}-Zn(1)-N(9)	111.30(11)	N(7)-Zn(1)-N(9)	100.09(11)
O(11)-Zn(2)-O(13)	111.68(11)	O(11)-Zn(2)-N(3)	108.83(11)
O(13)-Zn(2)-N(3)	111.88(11)	O(11)-Zn(2)-N(2)	102.39(11)
O(13)-Zn(2)-N(2)	122.76(10)	N(3)-Zn(2)-N(2)	97.85(11)

Symmetry code: ^{i} -x,-y-1,-z+1.

Table S6. Selected bond lengths [Å] and angles [deg] for **5**.

5			
Zn(1)-O(9)	1.9105(17)	Zn(1)-O(10)	1.9358(17)
Zn(1)-N(8)	2.029(2)	Zn(1)-N(6)	2.038(2)
Zn(2)-O(9)	1.9197(18)	Zn(2)-O(11)	1.9365(17)
Zn(2)-N(4)	2.020(2)	Zn(2)-N(2)	2.037(2)
O(9)-Zn(1)-O(10)	110.82(8)	O(9)-Zn(1)-N(8)	109.14(9)
O(10)-Zn(1)-N(8)	113.72(9)	O(9)-Zn(1)-N(6)	104.68(8)

O(10)-Zn(1)-N(6)	118.61(9)	N(8)-Zn(1)-N(6)	98.84(9)
O(9)-Zn(2)-O(11)	108.72(8)	O(9)-Zn(2)-N(4)	108.26(9)
O(11)-Zn(2)-N(4)	119.95(8)	O(9)-Zn(2)-N(2)	107.45(9)
O(11)-Zn(2)-N(2)	113.32(9)	N(4)-Zn(2)-N(2)	98.23(8)

Table S7. Selected bond lengths [Å] and angles [deg] for **6**.

6			
Zn(1)-O(9)	1.910(2)	Zn(1)-O(12)^{i}	1.9572(18)
Zn(1)-N(4)	2.016(2)	Zn(1)-N(6)	2.028(2)
Zn(2)-O(9)	1.915(2)	Zn(2)-O(10)	1.9268(19)
Zn(2)-N(2)	2.008(2)	Zn(2)-N(8)	2.025(2)
O(9)-Zn(1)-O(12)^{i}	105.63(9)	O(9)-Zn(1)-N(4)	109.04(10)
O(12)^{i}-Zn(1)-N(4)	124.43(9)	O(9)-Zn(1)-N(6)	107.54(9)
O(12)^{i}-Zn(1)-N(6)	110.29(9)	N(4)-Zn(1)-N(6)	98.94(10)
O(9)-Zn(2)-O(10)	112.48(9)	O(9)-Zn(2)-N(2)	107.50(10)
O(10)-Zn(2)-N(2)	111.95(9)	O(9)-Zn(2)-N(8)	107.85(10)
O(10)-Zn(2)-N(8)	115.79(10)	N(2)-Zn(2)-N(8)	100.34(11)

Symmetry code: ^{i} -x,-y,-z.

Table S8. Selected bond lengths [Å] and angles [deg] for **7**.

7			
Zn(1)-O(13)	1.906(4)	Zn(1)-O(10)^{i}	1.935(3)
Zn(1)-N(2)	2.019(4)	Zn(1)-N(4)	2.039(4)

Zn(2)-O(13)	1.921(3)	Zn(2)-O(11)	1.926(3)
Zn(2)-N(8)	2.023(4)	Zn(2)-N(6)	2.044(4)
O(13)-Zn(1)-O(10)^{i}	110.59(14)	O(13)-Zn(1)-N(2)	108.65(16)
O(10)^{i}-Zn(1)-N(2)	117.43(15)	O(13)-Zn(1)-N(4)	106.85(16)
O(10)^{i}-Zn(1)-N(4)	114.08(15)	N(2)-Zn(1)-N(4)	98.20(16)
O(13)-Zn(2)-O(11)	109.27(15)	O(13)-Zn(2)-N(8)	109.39(15)
O(11)-Zn(2)-N(8)	113.75(16)	O(13)-Zn(2)-N(6)	106.65(16)
O(11)-Zn(2)-N(6)	119.71(14)	N(8)-Zn(2)-N(6)	97.23(15)

Symmetry code: ^{i} -x+1,-y-1,-z+2.

Table S9. Selected bond lengths [Å] and angles [deg] for **8**.

8			
Zn(1)-O(13)	1.914(3)	Zn(1)-O(11)^{i}	1.936(2)
Zn(1)-N(6)	2.016(4)	Zn(1)-N(4)	2.040(3)
Zn(2)-O(13)	1.910(3)	Zn(2)-O(9)	1.932(3)
Zn(2)-N(8)	2.019(3)	Zn(2)-N(2)	2.044(4)
O(13)-Zn(1)-O(11)^{i}	110.33(12)	O(13)-Zn(1)-N(6)	108.54(14)
O(11)^{i}-Zn(1)-N(6)	118.06(13)	O(13)-Zn(1)-N(4)	107.11(14)
O(11)^{i}-Zn(1)-N(4)	113.59(12)	N(6)-Zn(1)-N(4)	98.21(14)
O(13)-Zn(2)-O(9)	110.04(12)	O(13)-Zn(2)-N(8)	109.38(14)
O(9)-Zn(2)-N(8)	113.96(13)	O(13)-Zn(2)-N(2)	106.66(14)
O(9)-Zn(2)-N(2)	118.91(14)	N(8)-Zn(2)-N(2)	96.94(14)

Symmetry code: ^{i} -x,-y+1,-z+1.

Table S10. Selected bond lengths [Å] and angles [deg] for **9**.

9			
Zn(1)-O(11)	1.9120(18)	Zn(1)-O(8)	1.9408(19)
Zn(1)-N(4)	2.015(2)	Zn(1)-N(2)	2.048(2)
Zn(2)-O(11)^{i}	1.919(2)	Zn(2)-O(10)	1.927(2)
Zn(2)-N(10)^{i}	2.024(2)	Zn(2)-N(6)^{i}	2.033(2)
O(11)-Zn(1)-O(8)	110.81(8)	O(11)-Zn(1)-N(4)	108.80(9)
O(8)-Zn(1)-N(4)	118.00(9)	O(11)-Zn(1)-N(2)	106.10(9)
O(8)-Zn(1)-N(2)	113.92(9)	N(4)-Zn(1)-N(2)	98.02(10)
O(11)^{i}-Zn(2)-O(10)	110.02(8)	O(11)^{i}-Zn(2)-N(10)^{i}	109.12(10)
O(10)-Zn(2)-N(10)^{i}	113.10(10)	O(11)^{i}-Zn(2)-N(6)^{i}	107.31(9)
O(10)-Zn(2)-N(6)^{i}	119.00(10)	N(10)^{i}-Zn(2)-N(6)^{i}	97.40(9)

Symmetry code: ^{i} -x+1,-y-1,-z+1.

Table S11. Hydrogen Bonds for Compounds **1-9** (Å and °).

Compounds	D-H···A	d(D-H)	d(H...A)	d(D...A)	<(DHA)
1	C48-H48···O7^{ii}	0.93	2.50	3.087(5)	121.1
	C51-H51···O8^{ii}	0.93	2.53	3.228(5)	132.0
2	C45-H45···O6^{ii}	0.93	2.52	3.103(4)	120.8
	C49-H49···O5^{ii}	0.93	2.63	3.287(4)	128.0
3	C43-H43···O8^{ii}	0.93	2.55	3.148(10)	112.5
	C48-H48···O7^{ii}	0.93	2.64	3.338(11)	132.7
4	C42-H42···O3^{ii}	0.93	2.39	3.112(4)	134.8
	C44-H44···O4^{ii}	0.93	2.57	3.302(4)	136.4
	C28-H28A···O12^{ii}	0.97	2.66	3.266(2)	120.5
5	C31-H31···O3^{i}	0.93	2.44	3.074(3)	125.4

	C33-H33···O4^{i}	0.93	2.69	3.372(2)	130.5
	C70-H70A···O12^{i}	0.97	2.70	3.367(2)	126.4
6	C37-H37···N9^{ii}	0.93	2.54	3.328(4)	143.1
	C52-H52···O2^{ii}	0.93	2.68	3.346(2)	129.01
	C48-H48···N6^{iii}	0.93	2.50	3.274(5)	140.7
7	C90-H90···O5^{ii}	0.93	2.45	3.093(6)	126.7
	C92-H92···O6^{ii}	0.93	2.48	3.202(6)	134.4
	C31-H31A···O9^{ii}	0.97	2.67	3.328(1)	125.6
8	C52-H52···O4^{ii}	0.93	2.48	3.181(5)	132.6
	C39-H39···O3^{ii}	0.93	2.46	3.079(5)	124.3
	C28- H28A···O10^{ii}	0.97	2.72	3.390(1)	126.4
9	C30-H30B···O9^{ii}	0.97	2.65	3.323(3)	126.5
	C42-H42···O5^{iii}	0.93	2.46	3.094(4)	125.8
	C85-H85···O6^{iii}	0.93	2.55	3.251(4)	132.8

Symmetry code for **1**: ^{ii} -1+x, y, z; symmetry code for **2**: ^{ii} -x+1, -y, -z+2; symmetry code for **3**: ^{ii} -x+1, -y+1, -z+1; symmetry code for **4**: ^{ii} x-1, y, z; symmetry code for **5**: ^{i} x+1, y, z; symmetry code for **6**: ^{ii} x+1, y, z; ^{iii} -x+1/2, y+1/2, -z+1/2. symmetry code for **7**: ^{ii} x+1, y, z; symmetry code for **8**: ^{ii} -1+x, y, z; symmetry code for **9**: ^{ii} -x, -y-1, -z+1; ^{iii} x+1, y, z.

References

(1) Wang, F.-F.; Liu, Y.-Y.; Pei, W.-Y.; Ma, J.-F. Three Resorcin[4]arene-Based 2D Zn(II) Supramolecular Isomers Synthesized via Structure-Directing Strategy for Knoevenagel Condensation. *Inorg. Chem.*, **2021**, *60*, 7329–7336.

(2) Sheldrick, G. M. SHELXS-2018, Programs for X-ray Crystal Structure Solution; University of Göttingen: Göttingen, Germany, **2018**.

(3) Farrugia, L. J. WINGX: A Windows Program for Crystal Structure Analysis; University of Glasgow: Glasgow, UK, **1988**.

(4) Sheldrick, G. M. SHELXTL-2018, Programs for X-ray Crystal Structure Refinement; University

of Göttingen: Göttingen, Germany, **2018**.

(5) Spek, A. L. PLATON SQUEEZE: A Tool for the Calculation of the Disordered Solvent Contribution to the Calculated Structure Factors. *Acta Crystallogr. Sect. C: Struct. Chem.*, **2015**, *71*, 9–18.

(6) Dong, S. H.; Liu, Z.; Liu, R. H.; Chen, L. M.; Chen, J. Z.; Xu, Y. S. Visible-Light-Induced Catalytic Transfer Hydrogenation of Aromatic Aldehydes by Palladium Immobilized on Amine-Functionalized Iron-Based Metal−Organic Frameworks. *ACS Appl. Nano Mater.*, **2018**, *1*, 4247–4257.